https://doi.org/10.5194/egusphere-2024-3793
Preprint. Discussion started: 6 January 2025

Contributions of primary anthropogenic sources and rapid secondary transformations to organic aerosol pollution in Nanchang, Central China

Wei Guo[a, b], Zicong Li[a, b], Renguo Zhu[a, b], Zhongkui Zhou[a], Hongwei Xiao[c], Huayun Xiao[c]

a. School of Water Resources and environmental Engineering, East China University of Technology, Nanchang 330013, China

b. Jiangxi Province Key Laboratory of the Causes and Control of Atmospheric Pollution, East China University of Technology, Nanchang 330013, China

c. School of Agriculture and Biology, Shanghai Jiao Tong University, Shanghai 200240, China

Correspondence: Huayun Xiao (xiaohuayun@sjtu.edu.cn)

Abstract

Owing to the complex composition of organic aerosols (OAs), it is challenging to elucidate their sources and dynamics, particularly in urban environments in China, where natural and anthropogenic influences converge. We attempted to clarify the relative contributions of primary emissions and secondary formations to urban OAs and confirm the sources and influencing factors of OA pollution. To achieve this, we conducted a comprehensive analysis of major polar organic compounds in fine particulate matter ($PM_{2.5}$) samples collected over a year in Nanchang, Central China. The results indicated that the concentrations of fatty acids, fatty alcohols, and saccharides were relatively high, whereas lignin and resin products, sterols, glycerol, hydroxy acids, and aromatic acids were present at low concentrations. An analysis of molecular characteristics and concentration ratios revealed that they originate from anthropogenic and natural sources. Using the tracer-based method, we observed that the primary organic carbon (POC) and primary organic aerosols (POA) contributed 53% of OC and 21% of $PM_{2.5}$ mass, respectively, compared with a mere 8% and 4% from secondary organic carbon (SOC) and secondary organic aerosols (SOA). Anthropogenic sources were the most dominant determinant, contributing approximately 89% of POC and POA and 60% of SOC and SOA. Seasonal variations indicated that biogenic emissions exerted a stronger influence during spring and summer, whereas anthropogenic emissions were more pronounced in autumn and winter. Short-term winter pollution

https://doi.org/10.5194/egusphere-2024-3793
Preprint. Discussion started: 6 January 2025

episodes were characterized by rapid secondary transformation, promoted by elevated primary emissions and favorable oxidation conditions, including increased light intensity and nitrogen oxides.

1 Introduction

Fine particulate matter (PM), specifically those with an aerodynamic diameter less than 2.5 μm ($PM_{2.5}$), affects the environment and climate, posing severe threats to human health (Huebert et al., 2003; Kanakidou, 2005; Riipinen et al., 2012; Shiraiwa et al., 2017; Yazdani et al., 2021). This is evident in China, which has become a focal point for $PM_{2.5}$ pollution, characterized by recurrent haze episodes that have intensified since 2011 (Cao et al., 2012; Zhang et al., 2012; Huang et al., 2014). To tackle this pressing challenge, the Chinese government implemented the "Air Pollution Prevention and Control Action Plan" in 2013, revisions to the "Air Pollution Prevention and Control Law" in 2014, and the "Three-year Action Plan for Winning the Blue Sky Defense War" in 2018. Such initiatives have significantly reduced $PM_{2.5}$ levels, with concentrations below 35 μg m^{-3} as of 2020. However, the challenge persists, particularly during winter, as exemplified by the winter of 2023–2024, when $PM_{2.5}$ concentrations in many cities exceeded the national air quality standards (Figures 1a and S1). This underscores an urgent need for effective air quality management strategies (An et al., 2019; Cao and Cui, 2021; Chen et al., 2021; Wu et al., 2021; Zhang et al., 2024). To address urban $PM_{2.5}$ pollution, a comprehensive investigation of pollutant components, an identification of pollution sources, and an evaluation of influencing factors are required.

Organic components make up an important part of $PM_{2.5}$, accounting for 30%–50% of its mass, with primary and secondary sources (Huang et al., 2014; Zhang et al., 2016; Haque et al., 2022). Primary organic carbon (POC) or primary organic aerosol (POA) is directly emitted from various sources, including biomass burning, coal combustion, vehicle exhaust, cooking, plant debris, and fungal spores (Guo et al., 2012; Yazdani et al., 2021). Secondary organic carbon (SOC) or secondary organic aerosol (SOA) forms in the atmosphere through the photooxidation of biogenic and anthropogenic volatile organic compounds (BVOCs and AVOCs) (Lewandowski et al., 2008; Stone et al., 2009). Common biogenic precursors include hemiterpenes, monoterpenes, and sesquiterpenes, whereas typical anthropogenic precursors include toluene and polycyclic aromatic hydrocarbons (PAHs) (Claeys et al., 2004; Al-Naiema and Stone, 2017; Jaoui et al., 2019). Owing to

https://doi.org/10.5194/egusphere-2024-3793
Preprint. Discussion started: 6 January 2025

the complex composition of OAs, their diverse emission sources, and the impact of meteorological conditions and photochemical oxidation processes, the identification of OA sources is complicated (Ding et al., 2013; Zhang et al., 2024). For years, research on the composition and source apportionment of OAs has attracted considerable attention. However, a unified conclusion regarding OA sources, particularly in China's intricate urban environments influenced by natural and anthropogenic factors, remains elusive (Wang et al., 2006; Fu et al., 2008; Guo et al., 2012; Ding et al., 2014; Xu et al., 2022). Various source apportionment methods have been employed. Such methods include the elemental carbon and water-soluble OC methods (EC-based and WSOC-based method; Xu et al., 2021), compound tracer method (tracer-based method; Ding et al., 2014; Ren et al., 2021; Haque et al., 2023), isotope signature method (Tang et al., 2022; Xu et al., 2022 and 2023; Zhang et al., 2024), and source apportionment models, such as the chemical mass balance (CMB) and positive matrix factorization models (Xu et al., 2021; Zhang et al., 2023). However, these methods yielded different source contributions. The relative significance of primary emissions versus secondary formation in urban OAs continues to be controversial. Further investigation is required to clarify the sources of OA pollution and the influencing factors.

Thus, this paper presents a comprehensive assessment of OAs in Nanchang, a city in Central China characterized by moderate $PM_{2.5}$ pollution levels that reflect broader urban atmospheric conditions across China. Employing the EC- and tracer-based methods, as well as the CMB model, we quantitatively evaluated the contributions of POC and SOC to OC, as well as the contributions of the corresponding POA and SOA to the mass of $PM_{2.5}$. The results showed that urban OAs were predominantly influenced by anthropogenic sources, with primary contributions exceeding secondary contributions. Based on a continuous year-long observation (November 1, 2020 to October 31, 2021, 365 daily samples), we discovered that the anthropogenic contributions significantly increased in autumn and winter. However, the biogenic contributions increased in spring and summer. Short-term winter pollution episodes were promoted by rapid secondary transformation, primarily due to high primary emissions and favorable oxidation conditions, including increased light intensity and nitrogen oxides (NO_x). This study integrates multiple source apportionment methods and accounts for the seasonal characteristics of OA pollution, providing a robust framework for understanding urban air quality dynamics. The findings have implications for governmental strategies for mitigating air pollution and

https://doi.org/10.5194/egusphere-2024-3793
Preprint. Discussion started: 6 January 2025

preventing haze episodes in Nanchang and its environs. The insights obtained serve as a future reference for investigating the impacts of organic compounds in $PM_{2.5}$ on visibility, public health, and climate change.

2 Materials and methods

2.1 Sampling sites and sample collection

The study area was Nanchang, Central China, with sampling at the East China University of Technology (ECUT) located in the northwest region of the city (28.72°N, 115.83°E; Figure 1b). As detailed in our previous investigations (Guo et al., 2024a and 2024b), the sampling site was in a mixed-use area characterized by educational, commercial, transportation, and residential activities, devoid of significant local pollution sources. The sampler was strategically placed on the rooftop of a six-story building, approximately 20 m in height, ensuring an unobstructed sampling environment.

Sampling was conducted from November 1, 2020, to October 31, 2021, with daily $PM_{2.5}$ sample collection. An 8-inch × 10-inch quartz fiber filter (Pall Tissuquartz, USA) was used in a high-volume air sampler for sample collection. The meteorological parameters and gaseous pollutant data for the sampling period were sourced from publicly available online monitoring platforms (https://weatherandclimate.info and http://www.aqistudy.cn/). Text S1 and Figure S2 provide a comprehensive overview of the prevalent meteorological conditions and air quality during the sampling period.

2.2 Chemical analyses

The OC and EC concentrations in the $PM_{2.5}$ samples were quantified using the Desert Research Institute Model 2001 Carbon Analyzer, following the thermal/optical reflectance protocol established by the Interagency Monitoring of Protected Visual Environments (IMPROVE). A 1.0-cm^2 filter sample was placed in a quartz boat in the analyzer and subjected to incremental heating at predetermined temperatures. Repeated analyses were performed, demonstrating an analytical uncertainty of ±10%.

We employed methodologies outlined by Wang et al. (2005, 2006) and Fu et al. (2008, 2010) for the extraction and derivatization of organic compounds. The filter samples underwent three consecutive ultrasonic extractions using a dichloromethane–methanol mixture (2:1 v/v), followed by the concentration and drying of the resulting extracts. Prior to instrumental analyses, N,O-bis-(trimethylsilyl) trifluoroacetamide and pyridine were introduced to derivatize the polar compounds in the extract, with C13 n-alkanes added as internal

https://doi.org/10.5194/egusphere-2024-3793
Preprint. Discussion started: 6 January 2025

standards for quantitative analyses.

The identification and quantification of organic compounds were achieved via gas chromatography-mass spectrometry (GC-MS), using a Thermo Scientific TRACE GC coupled to a Thermo Scientific ISQ QD single quadrupole mass spectrometer. GC separation was performed using a DB-5MS fused silica capillary column. Text S2 and Table S1 present the parameters for the GC-MS analysis, including temperature elevation procedures, qualitative and quantitative methods for the compounds, and quality assurance and control protocols. Polar and nonpolar organic compounds in the extracts were simultaneously analyzed; however, this study focused on the results regarding the polar compounds; the findings related to nonpolar compounds are provided in our earlier publications (Guo et al., 2024a and 2024b).

2.3 Source apportionment methods

To assess the contributions of various primary and secondary sources to OC and $PM_{2.5}$, we employed the tracer-based approach, a well-established method for source apportionment. This study focused on two types of organic tracers that serve as indicators for POC and SOC or POA and SOA. By integrating the reported ratios of specific tracers to OC and aerosol mass concentrations from various emission sources with the actual tracer concentrations measured in the present samples, we calculated the contributions of these sources to OC and $PM_{2.5}$. The calculation equation was as follows (Kleindienst et al., 2007 and 2012):

$$[POC]=\frac{\sum_i[tr_i]}{f_{POC}}, \quad (1)$$

$$[POA]=\frac{\sum_i[tr_i]}{f_{POA}}, \quad (2)$$

$$[SOC]=\frac{\sum_i[tr_i]}{f_{SOC}}, \quad (3)$$

$$[SOA]=\frac{\sum_i[tr_i]}{f_{SOA}}, \quad (4)$$

where $\sum i[tri]$ is the total concentration of the selected tracers in the sample, denoting representative compounds from specific emission categories; f_{POC} and f_{POA} are the mass fractions of the tracers in OC and

https://doi.org/10.5194/egusphere-2024-3793
Preprint. Discussion started: 6 January 2025

$PM_{2.5}$ from primary emissions, respectively. Similarly, f_{SOC} and f_{SOA} are the mass fractions of the tracers in OC and $PM_{2.5}$ from secondary emissions, respectively. The calculated [POC], [POA], [SOC], and [SOA] are the contributions of different primary and secondary sources to OC and $PM_{2.5}$. Here, we identified mass fractions for representative tracers from several significant primary and secondary emission sources. The primary sources included biomass burning, coal combustion, vehicle exhaust, cooking activities, plant debris, and fungal spores. The secondary sources were categorized into biogenic (isoprene, monoterpenes, and sesquiterpenes) and anthropogenic (toluene and naphthalene) sources. Table S2 presents information on the representative tracers, their corresponding f_{OC} and f_{OA}, and relevant references.

We employed the CMB model (version 8.2) provided by the US Environmental Protection Agency to verify the results calculated using the tracer-based method. This model assumes a CMB between the emission sources and environmental receptors. Thus, the mass of pollutants is not lost during transport from the source to the receptor, and the measured chemical component concentration at the receptor is the linear superposition of the contribution of each source class to the concentration (Stone et al., 2009). Furthermore, we employed the EC-based method to estimate the total POC and SOC concentrations, enabling a comparison with the POC and SOC concentrations obtained via the tracer-based approach. This method uses EC as a tracer for POC and approximates the observed minimum ratio of OC to EC $(OC/EC)_{min}$ as an equivalent to the primary emission OC/EC value $(OC/EC)_{pri}$ (Turpin and Huntzicker, 1995; Castro et al., 1999). The equation used for estimating SOC is

$$SOC_{EC\text{-}based} = OC - EC \times (OC/EC)_{min}. \quad (5)$$

Here, the minimum OC/EC values observed in spring, summer, autumn, and winter were 2.01, 2.20, 2.15, and 2.31, respectively.

3 Results and discussion

3.1 Carbonaceous components

The OC and EC concentrations were in the ranges of 1.01–13.66 μg m^{-3} (mean: 5.88 ± 2.57 μg m^{-3}) and 0.27–4.55 μg m^{-3} (mean: 1.75 ± 0.88 μg m^{-3}), respectively. Seasonal variations in the OC and EC concentrations closely mirrored those observed for $PM_{2.5}$, with elevated levels in autumn and winter, and diminished levels in spring and summer (Figure 2). The OC/EC ratio is a widely employed metric for characterizing emissions from

https://doi.org/10.5194/egusphere-2024-3793
Preprint. Discussion started: 6 January 2025

fossil fuels and biomass combustion. OC/EC values below 1.1 typically indicate vehicle exhaust emissions; values within the range of 2–3 suggest coal combustion emissions, and values above 7 indicate biomass burning (Saarikoski et al., 2008). Here, the OC/EC range was 2.01–16.95, with an average of 3.86 ± 2.05. These OC/EC ratios fell within the ranges associated with coal and biomass burning emissions. This suggests that the carbonaceous material was predominantly derived from combustion. Furthermore, owing to its stability and resistance to chemical transformations in the atmosphere, EC is frequently used as a tracer for primary emissions. The OC/EC ratio is a useful tool for assessing the relative contributions of primary and secondary sources (Castro et al., 1999;Turpin and Huntzicker, 1995). Generally, an OC/EC value above 2 indicates a predominant contribution of secondary sources to OC, whereas values below 2 suggest greater contributions from primary sources (Kunwar and Kawamura, 2014). Here, the majority of the OC/EC values exceeded 2, implying that the OC may have been significantly influenced by secondary sources. The OC/EC values were relatively higher in summer (4.33 ± 2.07) and winter (4.18 ± 2.57) compared with those observed in spring (3.36 ± 1.98) and autumn (3.59 ± 1.22). This indicates an increased contribution to OC from secondary sources during the summer and winter.

3.2 Major polar components

3.2.1 Fatty acids

A range of homologous straight-chain C10:0–C32:0 fatty acids (FAs) and unsaturated C16:1 and C18:1 FAs were detected in the $PM_{2.5}$ samples (Figure 3a). Their distribution exhibited a strong even carbon number predominance, as indicated by a Carbon Preference Index (CPI) of 7.59 ± 7.42 (Figure 4a), with peaks at C16:0 and C18:0. The total FA concentration was in the range of 3.24–657.86 ng m^{-3}, with an average concentration of 196.50 ± 110.92 ng m^{-3}. Similar molecular distribution patterns and concentrations have been documented in urban aerosol studies across China (59–2,090 ng m^{-3}; Wang et al., 2006; Fu et al., 2008; Haque et al., 2019; Fan et al., 2020). This average concentration generally exceeds those observed for coastal and marine aerosol samples (0.1–160 ng m^{-3}; Kawamura et al., 2003; Wang et al., 2007; Fu et al., 2011). High molecular weight FAs (HFAs, ≥ C20:0) are typically derived from the waxes of terrestrial higher plants or biomass burning, whereas low molecular weight FAs (LFAs, < C20:0) originate from more diverse sources, including vascular plants, microorganisms, marine phytoplankton, and kitchen emissions (Fu et al., 2010).

https://doi.org/10.5194/egusphere-2024-3793
Preprint. Discussion started: 6 January 2025

Consequently, the ratio of LFAs to HFAs (LFAs/HFAs) is an indicator of the relative contributions from various sources. Here, the LFA/HFA range was 0.34–10.67, with an average of 2.45 ± 1.53 (Figure 4b), suggesting that the FAs may have originated from a mixture of natural and anthropogenic sources. The specific FAs C16:0 and C18:0 are associated with different sources. C16:0 is primarily derived from biomass burning or plant emissions, whereas C18:0 predominantly originates from vehicle exhaust, cooking emissions, or road dust (Wang et al., 2007; Fu et al., 2010). Thus, the ratio of C18:0 to C16:0 (C18:0/C16:0) is frequently used to assess the FA source. A C18:0/C16:0 ratio below 0.25 suggests a primary contribution from biomass burning or plant emissions, whereas ratios between 0.25 and 0.5 indicate a predominant influence from vehicle exhaust. C18:0/C16:0 ratios within the range of 0.5–1 suggest a significant contribution from cooking emissions or road dust (Rogge et al., 2006). Here, the C18:0/C16:0 varied from 0.05 to 9.53, with an average of 0.59 ± 0.88 (Figure 4c), indicating that the FAs in Nanchang originated from a mixture of sources.

The average concentrations of unsaturated FAs, specifically C16:1 and C18:1, were 6.94 ± 4.35 and 3.79 ± 2.86 ng m^{-3}, respectively. Such unsaturated FAs are primarily derived from biomass burning, plant leaf emissions, cooking activities, and release from marine organisms (Kawamura and Gagosian, 1987; Rogge et al., 1993; Nolte et al., 1999). Upon emission into the atmosphere, unsaturated FAs undergo rapid oxidation by ozone (O_3), hydrogen peroxide (H_2O_2), or hydroxyl (OH) radicals. Consequently, the ratio of unsaturated FAs to saturated FAs, represented as (C16:1 + C18:1)/(C16:0 + C18:0), is an indicator of the reactivity and degree of aging of unsaturated FAs (Rudich et al., 2007; Kawamura and Gagosian, 1987). Here, this ratio was 0.12 ± 0.06 (Figure 4d), indicating that the unsaturated FAs underwent significant photochemical degradation and that secondary organic compounds may be common in $PM_{2.5}$.

The LFAs/HFAs and C18:0/C16:0 were relatively low during autumn and winter compared with spring and summer (Figures 4b and 4c). This indicated that in autumn and winter, FAs were significantly influenced by terrestrial plant or biomass burning, whereas in spring and summer, they were more influenced by vehicular emissions, marine phytoplankton, and cooking emissions. Conversely, the (C16:1 + C18:1)/(C16:0 + C18:0) values were relatively higher in autumn and winter than in spring and summer (Figure 4d). This suggested that unsaturated FAs experienced a greater degree of photochemical degradation during the warm seasons.

3.2.2 Fatty alcohols

https://doi.org/10.5194/egusphere-2024-3793
Preprint. Discussion started: 6 January 2025

A series of straight-chain n-alkanols (C14–C32) were detected (Figure 3b), exhibiting a predominance of even carbon numbers, as indicated by a CPI of 10.28 ± 17.05 (Figure 4e). Low molecular weight alcohols (LMW_{alc}, ≤ C20) exhibited peaks at C16 and C18, and high MW alcohols (HMW_{alc}, > C20), exhibited peaks at C26, C28, and C30 (Figure 3b). The total concentration of n-alkanols was in the range of 5.80–572.01 ng m^{-3} (average = 113.99 ± 92.50 ng m^{-3}). This concentration fell within the range of reported n-alkanol concentrations in urban aerosols in China (3.1–1,301.0 ng m^{-3}; Wang et al., 2006; Fu et al., 2008; Haque et al., 2019; Fan et al., 2020) and generally exceeded that of coastal and marine aerosol samples (0.1–19.7 ng m^{-3}; Kawamura et al., 2003; Fu et al., 2011). HMW_{alc} mainly originates from higher plant leaf waxes, loess deposits, or biomass burning, and LMW_{alc} primarily originates from soil and marine microorganisms (Simoneit, 2002; Kawamura et al., 2003). Here, the LMW_{alc} concentration (75.12 ± 61.28 ng m^{-3}) relatively exceeded that of HMW_{alc} (39.09 ± 34.07 ng m^{-3}), yielding an average LMW/HMW of 2.50 ± 1.73 (Figure 4f), indicating a mixture of n-alkanols from soil, marine organisms, and biomass burning. The LMW/HMW values were relatively lower in autumn and winter and higher in spring and summer (Figure 4f). This suggests an increased contribution of soil and marine organisms to n-alkanols in spring and summer. Contributions from plant or biomass burning increased in autumn and winter.

3.2.3 Saccharides

We investigated three saccharide classes: anhydrosugars, primary sugars, and sugar alcohols. Among the anhydrosugars, levoglucosan had the highest concentration (102.48 ± 78.63 ng m^{-3}). We observed markedly lower concentrations of mannosan (4.33 ± 4.04 ng m^{-3}) and galactosan (2.41 ± 2.67 ng m^{-3}) (Figure 3c). Levoglucosan, a prominent biomarker for biomass burning, has been extensively investigated in urban aerosol samples, with concentrations in the range of 22–2,706 ng m^{-3} (Wang and Kawamura, 2005; Wang et al., 2006; Fu et al., 2010; Haque et al., 2019; Fan et al., 2020), indicating the significant influence of biomass burning on the urban atmosphere. The widespread detection of levoglucosan across diverse environments, including suburban (10–482 ng m^{-3}; Yttri et al., 2007; Fu et al., 2008), marine (0.2–30 ng m^{-3}; Simoneit et al., 2004a; Fu et al., 2011), and polar (0–3 ng m^{-3}; Stohl et al., 2007; Fu et al., 2009) regions, suggests its potential for long-range atmospheric transport. Seasonal variations of anhydrosugars exhibited consistent patterns, with elevated concentrations in autumn and winter and reduced levels in spring and summer (Figure 3c). This indicated

https://doi.org/10.5194/egusphere-2024-3793
Preprint. Discussion started: 6 January 2025

increased biomass burning during the cold months. The sources were characterized using levoglucosan-to-mannosan (L/M) and mannosan-to-galactosan (M/G) ratios. Research suggests distinct L/M ranges for different biomass-burning sources: softwood (3–10), hardwood (13–35), and agricultural crop burning (40–56) (Oros and Simoneit, 2001; Sheesley et al., 2003; Engling et al., 2014). Coal combustion can produce significant amounts of levoglucosan (Sheesley et al., 2003; Fabbri et al., 2009), typically with higher L/M values (12–189) because of the lower cellulose content compared with that of plant materials (Rybicki et al., 2020a and 2020b). Conversely, M/G values are generally higher for softwood and hardwood combustion at 3.6–7.0 and 1.2–2.0, respectively. However, M/G values are relatively lower for agricultural crop burning (0.3–0.6) (Oros and Simoneit, 2001; Sheesley et al., 2003). Here, most samples exhibited relatively high L/M ratios (4.63–466.61, average = 40.22 ± 49.82), and relatively low M/G ratios (0.30–9.41, average = 2.34 ± 1.36). The L/M and M/G ratios were similar to those of previous observations in the urban area of Nanchang (L/M = 7.9–359.1; average = 59.9; Zhu et al., 2022) and fell within the ranges for crop residue burning and coal combustion. This suggests that the dehydrosugars in the $PM_{2.5}$ of Nanchang were likely primarily derived from crop residue burning and coal combustion. In the autumn and winter, the contributions of crop residue burning and coal combustion were more prominent, as evidenced by the higher L/M ratios and lower M/G ratios observed compared with those in the spring and summer (Figures 4g and 4h).

Primary sugars and sugar alcohols serve as tracers for primary biological aerosol particles, originating from biogenic emissions, including the release of microorganisms, plants, and flowers, as well as the resuspension of surface soils and unpaved road dust containing biological materials (Graham et al., 2003; Simoneit et al., 2004b;Yttri et al., 2007). Furthermore, biomass burning is a significant source of primary sugars and sugar alcohols (Fu et al., 2012). We identified nine primary sugars (ribose, fructose, galactose, glucose, sucrose, lactulose, maltose, turanose, and trehalose; Figure 3c). Glucose (14.90 ± 6.62 ng m^{-3}) and sucrose (14.68 ± 6.48 ng m^{-3}) exhibited the highest concentrations, followed by fructose (10.82 ± 4.54 ng m^{-3}), trehalose (7.92 ± 4.40 ng m^{-3}), and maltose (5.39 ± 3.43 ng m^{-3}). The concentrations of galactose (1.88 ± 1.24 ng m^{-3}), ribose (2.87 ± 2.18 ng m^{-3}), turanose (0.87 ± 0.61 ng m^{-3}), and lactulose (0.83 ± 0.54 ng m^{-3}) were comparatively low. We detected four sugar alcohols (mannitol, arabitol, pinitol, and inositol). Mannitol (9.88 ± 4.57 ng m^{-3}) exhibited the highest concentration, followed by pinitol (6.05 ± 4.23 ng m^{-3}) and arabitol (4.96 ± 3.39 ng m^{-3}).

https://doi.org/10.5194/egusphere-2024-3793
Preprint. Discussion started: 6 January 2025

The concentration of inositol (2.05 ± 1.66 ng m^{-3}) was low.

Levoglucosan serves as a specific biomarker for biomass burning, enabling the assessment of biomass-burning contributions to sugar compounds through the ratio of levoglucosan to OC (Lev/OC) and the proportion of levoglucosan in the total sugar compounds (Lev%). Typically, a Lev/OC ratio above 0.048 and a Lev% above 68% indicate a dominance of biomass burning. Conversely, values below these thresholds suggest that, in addition to biomass burning, other sources, such as biogenic emissions, significantly contribute to the presence of sugar compounds (Yan et al., 2019 and references therein). Here, the Lev% and Lev/OC were 53.57% ± 17.93% and 0.016 ± 0.009 (Figures 4i and 4j), respectively, indicating that the sugar compounds were influenced by biomass burning and biogenic emissions, particularly the primary sugars and sugar alcohols. Primary sugars, such as glucose and trehalose, as well as the mannitol in sugar alcohol, positively correlated with levoglucosan (Figure S3a). This confirmed that biomass burning may be a potential source of primary sugars and sugar alcohols. However, the correlation was not statistically significant, suggesting that biological sources remain an important contributor to these compounds in Nanchang. The Lev/OC and Lev% values were higher in autumn and winter than in spring and summer (Figures 4i and 4j), further indicating that biomass-burning contributions increased during the cold months.

3.3 Minor polar components

3.3.1 Lignin, resin products, and sterols

Here, we detected four types of lignin and resin-derived compounds: 4-hydroxybenzoic acid, dehydroabietic acid, vanillic acid, and syringic acid (Figure 5a). These are generally considered to originate from natural plant release and burning. The burning of coniferous trees, such as pine, releases high concentrations of dehydroabietic acid compared with other lignin and resin-derived compounds (Simoneit, 2002). Here, the concentrations of 4-hydroxybenzoic acid (5.06 ± 3.57 ng m^{-3}) and dehydroabietic acid (2.98 ± 1.91 ng m^{-3}) were high, whereas those of vanillic acid (1.50 ± 1.08 ng m^{-3}) and syringic acid (1.53 ± 1.11 ng m^{-3}) were relatively low. A significant positive correlation was observed between the total concentration of lignin and resin-derived compounds and levoglucosan ($r = 0.80$, $p < 0.01$, Figure S3a), suggesting that biomass burning was a potential source of lignin and resin-derived compounds. The concentration of dehydroabietic acid was significantly lower than that of 4-hydroxybenzoic acid, similar to the pattern observed for Nanjing aerosols

https://doi.org/10.5194/egusphere-2024-3793
Preprint. Discussion started: 6 January 2025

(Haque et al., 2019). This implies that coniferous tree combustion may not be the primary source of lignin and resin acids in this region.

We identified several sterols (cholesterol, stigmasterol, and β-sitosterol, average concentrations = 4.63 ± 3.17, 4.89 ± 3.68, and 10.11 ± 8.26 ng m^{-3}, respectively; Figure 5a). These sterols originate from distinct sources. Cholesterol, an animal-derived sterol, is primarily associated with meat cooking in the atmosphere (Rogge et al., 1991; Nolte et al., 1999; He et al., 2004). Contrarily, stigmasterol and β-sitosterol are plant-derived sterols, typically originating from plant leaves, cooking, or biomass burning (Nolte et al., 2001; He et al., 2004; Zhao et al., 2007). Here, stigmasterol and β-sitosterol exhibited a significant positive correlation with levoglucosan (Figure S3a). This suggests that biomass burning may be a potential source of plant-derived sterols. The concentration of stigmasterol and β-sitosterol was higher in autumn and winter than in spring and summer, indicating an increased contribution of biomass burning to sterols in the autumn and winter.

3.3.2 Glycerol and hydroxy acids

Glycerol and three hydroxy acids, glycolic acid, malic acid, and citric acid, were detected in the $PM_{2.5}$ samples (Figure 5b). The concentration of glycerol was relatively high (9.99 ± 4.13 ng m^{-3}), whereas the three hydroxy acids exhibited comparable and relatively lower concentrations: glycolic acid (7.16 ± 1.90 ng m^{-3}), malic acid (6.60 ± 1.85 ng m^{-3}), and citric acid (5.92 ± 1.99 ng m^{-3}). These concentrations aligned with reported ranges for urban aerosols (2–146 and 1–180 ng m^{-3} for glycerol and hydroxy acids, respectively; Wang et al., 2006; Fu et al., 2010; Haque et al., 2019; Fan et al., 2020). The glycerol in the aerosol is primarily derived from fungal metabolism in suspended soil (Simoneit et al., 2004b), whereas glycolic, malic, and citric acids mainly originate from the secondary photooxidation of organic compounds in the atmosphere (Kawamura and Ikushima, 1993; Kawamura and Sakaguchi, 1999; Claeys et al., 2004). No significant correlation was observed between glycerol and the hydroxy acids; however, a notable correlation was observed among the hydroxy acids ($r = 0.49–0.66$, $p < 0.01$, Figure S3b). This confirmed the divergent sources of glycerol and hydroxy acids and similar origins for the hydroxy acids. In summer, the concentrations of the hydroxy acids exceeded those in other seasons (Figure 5b). A positive correlation was observed between the polyacids and temperature ($r = 0.35–0.51$, $p < 0.01$), suggesting enhanced secondary photochemical oxidation processes in the warm months.

3.3.3 Aromatic acids

https://doi.org/10.5194/egusphere-2024-3793
Preprint. Discussion started: 6 January 2025

We detected four aromatic acids in the $PM_{2.5}$ samples: benzoic acid, phthalic acid, isophthalic acid, and terephthalic acid at concentrations of 0.76 ± 0.34, 6.40 ± 4.05, 1.10 ± 0.74, and 10.06 ± 3.07 ng m^{-3}, respectively (Figure 5b). Aromatic acids significantly contribute to the formation of atmospheric particles. Benzoic acid is recognized as a major pollutant in vehicle exhaust and the secondary photochemical oxidation product of aromatic hydrocarbons from vehicle emissions (Kawamura and Kaplan, 1987; Rogge et al., 1993; Kawamura et al., 2000). Phthalic acid typically originates from the secondary transformation of PAHs, including naphthalene and other PAHs. Terephthalic acid is primarily produced through the hydrolysis of terephthalate during the combustion of urban plastics (Fu et al., 2010; Haque et al., 2019). Here, phthalic and terephthalic acids jointly accounted for approximately 90% of the total aromatic acids detected. A significant positive correlation was observed between phthalic acid and PAHs ($r = 83$, $p < 0.01$), as well as between terephthalic acid and the total phthalates ($r = 0.72$, $p < 0.01$). The PAH and phthalate data have been published by Guo et al. (2024a and 2004b). This suggests that the secondary conversion of PAHs and the hydrolysis of phthalates (specifically terephthalate) during plastic burning significantly contribute to aromatic acid levels. The phthalic acid concentrations were higher in autumn and winter, whereas terephthalic acid levels peaked in spring and summer (Figure 5b). This indicates that the secondary transformation of PAHs was more pronounced during the cold months, whereas high temperatures in spring and summer promoted the volatilization and transformation of phthalates from plastic sources.

3.4 Secondary organic aerosol tracers in $PM_{2.5}$

3.4.1 Biogenic secondary organic aerosol tracers

Biogenic and anthropogenic SOAs play critical roles in influencing the atmospheric radiation balance and regional air quality (Ding et al., 2014). Biogenic SOA tracers include oxidation products from isoprene, monoterpenes, sesquiterpenes, and other oxygenated hydrocarbons. Isoprene is the dominant component of BVOC emissions, accounting for approximately 45% of the total emissions (annual release estimated at 600 Tg C) (Piccot et al., 1992; Guenther et al., 1995; Sharkey et al., 2008). Here, we detected six isoprene oxidation products (2-methylglyceric acid (2-MGA), three C5-alkene triols, and two 2-methyltetrols (MTLs) at concentrations of 1.83 ± 1.11, 2.84 ± 1.88, and 4.14 ± 3.27 ng m^{-3}, respectively; Figure 6). The concentrations of the C5-alkene triols and MTLs exceeded that of 2-MGA. Generally, C5-alkene triols primarily originate

https://doi.org/10.5194/egusphere-2024-3793
Preprint. Discussion started: 6 January 2025

from the secondary transformation of VOCs released during biomass burning and higher plant waxes (Fu et al., 2010 and 2014). Throughout the sampling period, a strong linear correlation was observed between the MTLs and C5-alkene triols (R^2 = 0.82, P < 0.01), indicating their similar sources. Nevertheless, certain differences were observed in the formation processes of C5-alkene triols and MTLs. Both compounds are formed through the acid-catalyzed ring-opening reaction of isoprene epoxydiols (Surratt et al., 2006 and 2010); however, the formation of C5-alkene triols is enhanced in acidic aerosol environments (Yee et al., 2020). Here, the ratios of C5-alkene triols to MTLs (C5/MTLs) were elevated in autumn and winter compared with those observed in spring and summer (Figure 7a), suggesting that increased aerosol acidity in the cold months may facilitate the production of C5-alkene triols. C5-alkene triols and MTLs are believed to form via isoprene oxidation under low-NO_x conditions (Surratt et al., 2010; Lin et al., 2013). Contrarily, high concentrations of NO_x favor the further oxidation of isoprene to yield 2-MGA (Lin et al., 2013; Nguyen et al., 2015). Here, the 2-MGA/MTL ratios in autumn and winter exceeded those observed in spring and summer (Figure 7b), indicating that elevated NO_x concentrations in the autumn and winter may enhance the formation of 2-MGA. In MTLs, 2-methylthreitol and 2-methylerythritol (MTL1 and MTL2) exhibited a significant linear correlation (R^2 = 0.68, P < 0.01), indicating that they may originate from similar sources and/or share similar formation pathways. The ratio of MTL2 to MTLs (MTL2/MTLs) can reflect the transformation pathways of MTLs. The ratio of MTL2/MTLs = 0.35, 0.61, 0.76, and 0.90 corresponded to isoprene secondary transformation from biogenic sources, OH-rich conditions (low NO_x), NO_x-rich conditions, and liquid-phase oxidation by H_2O_2, respectively (Kleindienst et al., 2009; Nozière et al., 2011). The results showed that the MTL2/MTLs values in spring (0.64 ± 0.12) and summer (0.59 ± 0.11) were relatively low and closer to the values for biogenic sources and OH-rich secondary transformation. However, the values in autumn and (0.66 ± 0.10) winter (0.69 ± 0.06) were relatively high, approaching those for NO_x-rich secondary transformation and liquid-phase oxidation by H_2O_2. This indicates that in spring and summer, MTLs were more likely derived from biogenic sources and OH-rich secondary transformation, whereas in autumn and winter, a shift was observed toward NOx-rich secondary transformations and liquid-phase oxidation by H_2O_2.

Monoterpenes represent a crucial component of BVOC emissions, accounting for approximately 11% of the annual emissions, with an annual emission of 110 Tg C (Guenther et al., 1995). Here, we identified four

https://doi.org/10.5194/egusphere-2024-3793
Preprint. Discussion started: 6 January 2025

oxidation products of monoterpene (pinonic acid (PNA); pinic acid (PA); 3-methyl-1,2,3-butanetricarboxylic acid (MBTCA); and 3-hydroxyglutaric acid (3-HGA)) at concentrations of 1.69 ± 0.99, 1.47 ± 0.86, 0.79 ± 0.61, and 0.77 ± 0.52 ng m^{-3}, respectively (Figure 6). The concentrations of PNA and PA exceeded those of MBTCA and 3-HGA. PNA and PA are produced via the oxidation of α/β-pinene via reactions with O_3 and OH radicals, and the α/β-pinene detected in the aerosol samples is mainly derived from biomass burning and higher plant release (Hallquist et al., 2009; Eddingsaas et al., 2012; Zhang et al., 2015; Iyer et al., 2021). The predominance of PNA over PA is attributable to its relatively higher vapor pressure, consistent with previous findings (Fu et al., 2008 and 2010). PNA and PA are recognized as first-generation oxidation products of α-/β-pinene, whereas MBTCA represents a second-generation oxidation product formed via the further photooxidation of PNA and PA with OH radicals. The relative concentrations of such first- and second-generation oxidation products (M/P) reflect the oxidation degree and aging status of monoterpene compounds (Ding et al., 2014). Here, the M/P values were higher in spring (0.25 ± 0.11) and summer (0.32 ± 0.10) than in autumn (0.16 ± 0.09) and winter (0.24 ± 0.10). This suggests that higher temperatures and/or stronger radiation in spring and summer promoted the oxidation of monoterpene compounds (Figure 7d). The formation of 3-HGA is considered to occur via a ring-opening mechanism, probably linked to heterogeneous reactions of monoterpenes with irradiation in NO_x-rich environments (Jaoui et al., 2005; Claeys et al., 2007). The ratio of MBTCA to 3-HGA (MBTCA/3-HGA) can be used to distinguish monoterpenes, as the secondary transformation of α-pinene yields MBTCA at significantly higher rates relative to 3-HGA compared with β-pinene (Jaoui et al., 2005). Here, the annual MBTCA/3-HGA value was 1.18 ± 0.65, close to those observed in urban environments in the United States (0.81 ± 0.32) and China (0.68 ± 0.65) (Lewandowski et al., 2013;Ding et al., 2014). The MBTCA/3-HGA value was higher in spring (1.31 ± 0.66) and summer (1.45 ± 0.70) than in autumn (1.09 ± 0.72) and winter (0.88 ± 0.32). This suggests that the contribution of α-pinene to monoterpene was higher in spring and summer than in autumn and winter (Figure 7e). The ratio of the total isoprene to monoterpene oxidation products (Iso/Pine) was lower in autumn and winter than in spring and summer (Figure 7f), indicating that the higher temperatures in spring and summer favored isoprene release.

BVOC emissions include a class of sesquiterpene compounds, among which β-caryophyllene is the most abundant and frequently reported (Ding et al., 2014; Fan et al., 2020). β-caryophyllinic acid, a product of the

https://doi.org/10.5194/egusphere-2024-3793
Preprint. Discussion started: 6 January 2025

ozonolysis or photooxidation of β-caryophyllene, predominantly originates from biomass burning and natural plant emissions, including those from pine and birch trees (Helmig et al., 2006; Duhl et al., 2008). Here, β-caryophyllinic acid was detected at a concentration of 2.74 ± 1.92 ng m^{-3}. The β-caryophyllinic acid concentrations in autumn (3.16 ± 1.77 ng m^{-3}) and winter (4.63 ± 1.61 ng m^{-3}) exceeded those observed in spring (1.49 ± 0.68 ng m^{-3}) and summer (1.14 ± 0.47 ng m^{-3}) (Figure 6). The higher concentrations of caryophyllinic acid in autumn and winter may be associated with increased biomass burning and subsequent secondary transformation of β-caryophyllene. During the sampling period, a significant positive linear correlation was observed between β-caryophyllinic acid and levoglucosan, supporting this inference (R^2 = 0.66, $P < 0.01$).

3.4.2 Anthropogenic secondary organic aerosol tracers

Anthropogenic SOA tracers include hydroxy and aromatic acids, which primarily originate from the secondary transformation of AVOCs. Although global AVOC emissions are relatively modest at 110 Tg C yr^{-1} (Piccot et al., 1992) compared with BVOC emissions, which reach 1,150 Tg C yr^{-1} (Guenther et al., 1995), the contribution of anthropogenic sources to SOA is frequently more pronounced in urban environments because of the impact of human activities (von Schneidemesser et al., 2010; Ding et al., 2012; Li et al., 2019). AVOC emissions in urban settings can enhance the oxidation of BVOCs, promoting SOA formation (Carlton et al., 2010; Hoyle et al., 2011). Here, we identified two primary anthropogenic SOA tracers, 2,3-dihydroxy-4-oxopentanoic acid (DHOPA) and phthalic acid at concentrations of 1.73 ± 1.10 and 6.38 ± 4.05 ng m^{-3}, respectively (Figures 5 and 6). DHOPA and phthalic acid are recognized as important markers for anthropogenic SOAs, produced via the oxidation of toluene and PAHs, such as naphthalene (Kawamura and Ikushima, 1993; Kleindienst et al., 2007 and 2012). Their concentrations were significantly elevated during autumn and winter compared with spring and summer (Figures 5 and 6). This indicated a marked increase in the contribution of anthropogenic sources to SOA during the cold months.

3.5 Source apportionment of organic carbon and aerosol

Employing a tracer-based methodology, we quantified the contributions of POC and SOC to the total OC (Figure 8). The results showed that the POC and SOC concentrations were 3.22 ± 1.81 and 0.50 ± 0.32 μg m^{-3} (Figure 8a and 8b), accounting for 53.30% ± 12.53% and 8.33% ± 3.29% of the measured OC, respectively

https://doi.org/10.5194/egusphere-2024-3793
Preprint. Discussion started: 6 January 2025

(Figure 8f). These results were within the reported ranges of POC (5% to 76%) and SOC (3% to 56%) proportions reported in other studies (Stone et al., 2009; Guo et al., 2012; Fan et al., 2020; Xu et al., 2021; Haque et al., 2023). Anthropogenic sources, including biomass burning, coal combustion, motor vehicle emissions, and cooking, contributed the majority of POC (2.89 ± 1.72 μg m^{-3}, accounting for 88.98% ± 6.24%). Natural sources, such as plant debris and fungal spores, contributed relatively little (0.33 ± 0.17 μg m^{-3}, accounting for 11.01% ± 6.24%). For SOC, anthropogenic contributions (0.33 ± 0.25 μg m^{-3}, accounting for 60.67% ± 21.29%) exceeded biogenic contributions (0.17 ± 0.09 μg m^{-3}, accounting for 39.05% ± 21.15%). The concentrations and relative abundances of anthropogenic POC and SOC were higher in autumn and winter, whereas biogenic POC and SOC exhibited greater concentrations and relative abundances during spring and summer (Figures 8a, 8b, 8d, and 8e). These results underscore the significant influence of biogenic emissions during the warm months, whereas anthropogenic emissions exert a pronounced effect during the cold months. This situation is primarily attributed to the elevated temperatures, and increased solar radiation during the warm months facilitates VOC release from vegetation, thereby promoting biogenic POC emissions and SOC formation. Contrarily, the rise in anthropogenic POC emissions from biomass burning and coal combustion during the cold months fosters the development of anthropogenic SOC in the atmosphere. Similarly, using a tracer-based methodology, we quantified the contributions of POA and SOA to $PM_{2.5}$ (Figure S4). The findings indicated that POA and SOA contributed 6.13 ± 3.58 and 1.02 ± 0.63 μg m^{-3}, accounting for 21.02% ± 6.50% and 3.47% ± 1.41% of the observed $PM_{2.5}$ mass in Nanchang, respectively. The anthropogenic POA (5.50 ± 3.41 μg m^{-3}, accounting for 88.74% ± 6.46%) and SOA (0.65 ± 0.48 μg m^{-3}, accounting for 58.79% ± 21.30%) exceeded the natural POA (0.63 ± 0.33 μg m^{-3}, accounting for 11.26% ± 6.46%) and SOA (0.37 ± 0.20 μg m^{-3}, accounting for 40.93% ± 21.19%), respectively. The POA and SOA exhibited patterns analogous to those of POC and SOC, with greater contributions recorded in autumn and winter compared with spring and summer. The tracer-based method inherently bears a degree of uncertainty, primarily due to the variability in the mass fractions of representative tracers in OC and OA (f_{oc} and f_{oa}) in different observational studies. Nevertheless, this method has been widely employed to estimate the contributions of various primary and secondary sources to OC and aerosol, with relatively reasonable results. Additional observational studies to determine the representative tracers in emission sources and their mass

https://doi.org/10.5194/egusphere-2024-3793
Preprint. Discussion started: 6 January 2025

fractions in OC and OA are crucial to reducing this uncertainty (Oros and Simoneit, 2000; He et al., 2004; Zhao et al., 2007; Zhang et al., 2008; Kleindienst et al., 2012; Andreae, 2019).

We employed the CMB model to calculate the contributions of different sources of POC and SOC to OC. The results derived from the CMB approach were largely consistent with those obtained using the tracer-based method (Figure S5). The CMB model operates on principles analogous to the tracer-based method, relying on the mass fractions of characteristic tracers in OC and OAs from emission sources to ascertain the contributions of different sources (Stone et al., 2009). Thus, theoretically, the results generated by the CMB model should be consistent with those obtained from the tracer-based method. The present results confirmed that both methods exhibited similar reliabilities. We employed the EC-based method to estimate the total POC and SOC concentrations. Dissimilar to the tracer-based method, which quantifies partial POC and SOC concentrations from specific sources, the EC-based method simply partitions the OC into POC and SOC, which calculates the total POC and SOC concentrations. The results demonstrated that the overall trends of the total POC and SOC calculated by the EC-based method were consistent with those obtained via the tracer-based method (Figure S6).

3.6 Characteristics of organic aerosols during winter pollution

From an annual timescale perspective, anthropogenic POC and SOC are synchronous with the measured OC and observed $PM_{2.5}$ mass (Figure S6). Correlation analysis revealed that anthropogenic POC and SOC exhibited a significant positive correlation ($r = 0.72–0.80$, $P < 0.01$) with the measured OC (Figure 9a). Redundancy analysis revealed that anthropogenic POC and SOC significantly contributed (40%–65%, $P < 0.01$) to the variations in OC concentration (Figure 9a). This suggests that anthropogenic OC and SOC are important factors influencing changes in the OC and $PM_{2.5}$ mass throughout the sampling period. Variations in POC, SOC, OC, and $PM_{2.5}$ mass were associated with specific meteorological conditions and gaseous pollutant concentrations. For instance, high POC, SOC, OC, and $PM_{2.5}$ concentrations corresponded to elevated atmospheric pressure, reduced precipitation, and increased NO_2 concentrations (Figure S2). This suggests that meteorological conditions and gaseous pollutant concentrations could also influence POC, SOC, OC, and $PM_{2.5}$ mass.

However, winter presents a different scenario. During the entire winter pollution period and separate PM

https://doi.org/10.5194/egusphere-2024-3793
Preprint. Discussion started: 6 January 2025

pollution episodes, POC did not maintain good consistency with the changes in OC and $PM_{2.5}$ mass, whereas SOC remained synchronized with their variations (Figure S6). Correlation and redundancy analyses further revealed that source-specific SOC, derived using the tracer methods, and the total SOC, calculated using the EC-based method, exhibited significant positive correlations with the measured OC ($r > 0.6$, $P < 0.05$) and significantly contributed (>40%, $P < 0.05$) to their variations (Figures 9b–9k). These findings indicate that on shorter timescales, particularly during brief PM pollution episodes lasting several days, SOC was a critical factor influencing the OC and $PM_{2.5}$ mass. The increased SOC concentration may be associated with elevated temperatures and NO_x concentrations during winter pollution episodes. This inference was supported by a significant linear positive correlation between temperature, NO_2 concentrations, and SOC concentrations observed during several winter pollution episodes (Figure 10). An increase in short-term solar radiation intensity and oxidant levels have been shown to accelerate SOC formation (Fry et al., 2009; Ng et al., 2017; Li et al., 2018; Ren et al., 2019). Nevertheless, the contribution of POC should not be underestimated, as its levels remained relatively high throughout the winter. This elevated POC concentration can also promote SOC transformation (Weber et al., 2007; Carlton et al., 2010; Hoyle et al., 2011; Srivastava et al., 2022).

4 Conclusions

We investigated the composition and concentration of major polar organic compounds in $PM_{2.5}$ samples collected over a year in Nanchang, Central China. The results revealed relatively high concentrations of FAs, fatty alcohols, and saccharides, whereas lignin, resin products, sterols, glycerol, hydroxy acids, and aromatic acids were detected at low levels.

The study findings indicate that the organic components in the $PM_{2.5}$ of Nanchang are predominantly derived from anthropogenic and natural sources. Anthropogenic sources were the primary contributors to OC and OA, and primary sources contributed more than secondary sources. Throughout the sampling period, we observed that the anthropogenic contributions significantly increased during autumn and winter, whereas biogenic contributions increased in spring and summer.

This study highlights the critical role of anthropogenic POC and SOC in influencing atmospheric $PM_{2.5}$ pollution over an annual sampling period. During short-term pollution episodes in winter (lasting several days), the rapid secondary transformation emerged as the primary driver of OC increment and $PM_{2.5}$ pollution.

https://doi.org/10.5194/egusphere-2024-3793
Preprint. Discussion started: 6 January 2025

Elevated primary emissions and favorable oxidation conditions, such as increased light intensity and NO_x levels, were identified as key factors facilitating the rapid secondary transformation of OC during the winter pollution episodes.

The study findings underscore the necessity for targeted management strategies that consider primary and secondary anthropogenic emission sources across different seasons and pollution periods. Although the tracer-based methodology provided preliminary insights into the OC and OA from diverse sources, the study encountered inherent limitations in characteristic compound identification. The source apportionment analysis potentially underestimated contributions from unidentified primary and secondary sources because of the restricted range of tracers used. To address this, future research should prioritize comprehensive observational studies aimed at identifying representative molecular tracers across a broader spectrum of emissions and quantifying the precise mass fractions of such tracers in OC and OAs.

Data availability. The dataset for this paper is available upon request from the corresponding author (xiaohuayun@sjtu.edu.cn).

Competing interests. The authors declare that they have no conflict of interest.

Author contributions. Huayun Xiao conceptualized and designed the research. Sampling was conducted by Zicong Li, while laboratory analyses were carried out by Wei Guo, Zicong Li, and Renguo Zhu. Data interpretation was supported by Zhongkui Zhou and Hongwei Xiao. The manuscript was primarily written by Wei Guo, with contributions and consultations from all other authors.

Acknowledgements. We thank Ziyue Zhang and Liqin Cheng for their help with sampling and laboratory work. This study was supported by the National Natural Science Foundation of China (grant number 41863002); the Jiangxi Provincial Natural Science Foundation (grant number 20242BAB25193); the Open Foundation of Jiangxi Province Key Laboratory of the Causes and Control of Atmospheric Pollution, East

https://doi.org/10.5194/egusphere-2024-3793
Preprint. Discussion started: 6 January 2025

China University of Technology (grant number AE2209); and the Open Foundation of Yunnan Province Key Laboratory of Earth System Science, Yunnan University (grant number ESS2024002).

References

Al-Naiema, I. M., and Stone, E. A.: Evaluation of anthropogenic secondary organic aerosol tracers from aromatic hydrocarbons, Atmos. Chem. Phys., 17, 2053–2065, https://doi.org/10.5194/acp-17-2053-2017, 2017.

An, Z. S., Huang, R. J., Zhang, R. Y., Tie, X. X., Li, G. H., Cao, J. J., Zhou, W. J., Shi, Z. G., Han, Y. M., Gu, Z. L., and Ji, Y. M.: Severe haze in northern China: A synergy of anthropogenic emissions and atmospheric processes, Proc. Natl. Acad. Sci. U.S.A., 116, 8657–8666, https://doi.org/10.1073/pnas.1900125116, 2019.

Andreae, M. O.: Emission of trace gases and aerosols from biomass burning – an updated assessment, Atmos. Chem. Phys., 19, 8523–8546, https://doi.org/10.5194/acp-19-8523-2019, 2019.

Cao, J. J., and Cui, L.: Current Status, Characteristics and Causes of Particulate Air Pollution in the Fenwei Plain, China: A Review, J. Geophys.Res-Atmos., 126, e2020JD034472, https://doi.org/10.1029/2020JD034472, 2021.

Cao, J. J, Xu, H. M, Xu, Q., Chen, B. H., and Kan, H. D.: Fine particulate matter constituents and cardiopulmonary mortality in a heavily polluted Chinese city, Environ. Health Perspect., 120, 373–378, https://doi.org/10.1289/ehp.1103671, 2012.

Carlton, A. G., Pinder, R. W., Bhave, P. V., and Pouliot, G. A.: To What Extent Can Biogenic SOA be Controlled?, Environ. Sci. Technol., 44, 3376–3380, https://doi.org/10.1021/es903506b, 2010.

Castro, L. M., Pio, C. A., Harrison, R. M., and Smith, D. J. T.: Carbonaceous aerosol in urban and rural European atmospheres: estimation of secondary organic carbon concentrations, Atmos. Environ., 33, 2771–2781, https://doi.org/10.1016/S1352-2310(98)00331-8, 1999.

Chen, C. R., Zhang, H. X., Yan, W. J., Wu, N. N., Zhang, Q., and He, K. B.: Aerosol water content enhancement leads to changes in the major formation mechanisms of nitrate and secondary organic aerosols in winter over the North China Plain, Environ. Pollut., 287, 117625, https://doi.org/10.1016/j.envpol.2021.117625, 2021.

Cheng, Y. B., Ma, Y. Q., and Hu, D.: Tracer-based source apportioning of atmospheric organic carbon and the influence of anthropogenic emissions on secondary organic aerosol formation in Hong Kong, Atmos. Chem. Phys., 21, 10589–10608, https://doi.org/10.5194/acp-21-10589-2021, 2021.

https://doi.org/10.5194/egusphere-2024-3793
Preprint. Discussion started: 6 January 2025

565 Claeys, M., Graham, B., Vas, G., Wang, W., Vermeylen, R., Pashynska, V., Cafmeyer, J., Guyon, P., Andreae,
566 M. O., Artaxo, P., and Maenhaut, W.: Formation of Secondary Organic Aerosols Through Photooxidation
567 of Isoprene, Science, 303, 1173–1176, https://doi.org/doi:10.1126/science.1092805, 2004.
568 Claeys, M., Szmigielski, R., Kourtchev, I., Van der Veken, P., Vermeylen, R., Maenhaut, W., Jaoui, M.,
569 Kleindienst, T. E., Lewandowski, M., Offenberg, J. H., and Edney, E. O.: Hydroxydicarboxylic Acids:
570 Markers for Secondary Organic Aerosol from the Photooxidation of α-Pinene, Environ. Sci. Technol., 41,
571 1628–1634, https://doi.org/10.1021/es0620181, 2007.
572 Ding, X., Wang, X. M., Gao, B., Fu, X. X., He, Q. F., Zhao, X. Y., Yu, J. Z., and Zheng, M.: Tracer-based
573 estimation of secondary organic carbon in the Pearl River Delta, south China, J. Geophys. Res-Atmos., 117,
574 https://doi.org/10.1029/2011JD016596, 2012.
575 Ding, X., Wang, X. M., Xie, Z. Q., Zhang, Z., and Sun, L. G.: Impacts of Siberian Biomass Burning on
576 Organic Aerosols over the North Pacific Ocean and the Arctic: Primary and Secondary Organic Tracers,
577 Environ. Sci. Technol., 47, 3149–3157, https://doi.org/10.1021/es3037093, 2013.
578 Ding, X., He, Q. F., Shen, R. Q., Yu, Q. Q., and Wang, X. M.: Spatial distributions of secondary organic
579 aerosols from isoprene, monoterpenes, β-caryophyllene, and aromatics over China during summer, J.
580 Geophys. Res-Atmos., 119, 11877–811891, https://doi.org/10.1002/2014JD021748, 2014.
581 Duhl, T. R., Helmig, D., and Guenther, A.: Sesquiterpene emissions from vegetation: a review, Biogeosciences,
582 5, 761–777, https://doi.org/10.5194/bg-5-761-2008, 2008.
583 Eddingsaas, N. C., Loza, C. L., Yee, L. D., Chan, M., Schilling, K. A., Chhabra, P. S., Seinfeld, J. H., and
584 Wennberg, P. O.: α-pinene photooxidation under controlled chemical conditions-Part 2: SOA yield and
585 composition in low- and high-NO_x environments, Atmos. Chem. Phys., 12, 7413–7427,
586 https://doi.org/10.5194/acp-12-7413-2012, 2012.
587 Engling, G., He, J., Betha, R., and Balasubramanian, R.: Assessing the regional impact of indonesian biomass
588 burning emissions based on organic molecular tracers and chemical mass balance modeling, Atmos. Chem.
589 Phys., 14, 8043–8054, https://doi.org/10.5194/acp-14-8043-2014, 2014.
590 Fabbri, D., Torri, C., Simoneit, B. R. T., Marynowski, L., Rushdi, A. I., and Fabiańska, M. J.: Levoglucosan
591 and other cellulose and lignin markers in emissions from burning of Miocene lignites, Atmos. Environ., 43,
592 2286–2295, https://doi.org/10.1016/j.atmosenv.2009.01.030, 2009.
593 Fan, Y. B., Liu, C. Q., Li, L. J., Ren, L. J., Ren, H., Zhang, Z. M., Li, Q. K., Wang, S., Hu, W., Deng, J. J., Wu,
594 L. B., Zhong, S. J., Zhao, Y., Pavuluri, C. M., Li, X. D., Pan, X. L., Sun, Y. L., Wang, Z. F, Kawamura, K.,
595 Shi, Z. B., and Fu, P. Q.: Large contributions of biogenic and anthropogenic sources to fine organic

https://doi.org/10.5194/egusphere-2024-3793
Preprint. Discussion started: 6 January 2025

aerosols in Tianjin, North China, Atmos. Chem. Phys., 20, 117–137, https://doi.org/10.5194/acp-20-117-2020, 2020.

Fry, J. L., Kiendler-Scharr, A., Rollins, A. W., Wooldridge, P. J., Brown, S. S., Fuchs, H., Dubé, W., Mensah, A., dal Maso, M., Tillmann, R., Dorn, H. P., Brauers, T., and Cohen, R. C.: Organic nitrate and secondary organic aerosol yield from NO_3 oxidation of β-pinene evaluated using a gas-phase kinetics/aerosol partitioning model, Atmos. Chem. Phys., 9, 1431–1449, https://doi.org/10.5194/acp-9-1431-2009, 2009.

Fu, P. Q., Kawamura, K., Okuzawa, K., Aggarwal, S. G., Wang, G., Kanaya, Y., and Wang, Z.: Organic molecular compositions and temporal variations of summertime mountain aerosols over Mt. Tai, North China Plain, J. Geophys. Res-Atmos., 113, https://doi.org/10.1029/2008JD009900, 2008.

Fu, P. Q., Kawamura, K., and Barrie, L. A.: Photochemical and other sources of organic compounds in the Canadian high arctic aerosol pollution during winter-spring, Environ. Sci. Technol., 43, 286–292, https://doi.org/10.1021/es803046q, 2009.

Fu, P. Q., Kawamura, K., Pavuluri, C. M., Swaminathan, T., and Chen, J.: Molecular characterization of urban organic aerosol in tropical India: contributions of primary emissions and secondary photooxidation, Atmos. Chem. Phys., 10, 2663–2689, https://doi.org/10, 2663-2689, 10.5194/acp-10-2663-2010, 2010.

Fu, P. Q, Kawamura, K., and Miura, K.: Molecular characterization of marine organic aerosols collected during a round-the-world cruise, J. Geophys. Res-Atmos., 116, https://doi.org/10.1029/2011JD015604, 2011.

Fu, P. Q., Kawamura, K., Kobayashi, M., and Simoneit, B. R. T.: Seasonal variations of sugars in atmospheric particulate matter from Gosan, Jeju Island: Significant contributions of airborne pollen and Asian dust in spring, Atmos. Environ., 55, 234–239, https://doi.org/10.1016/j.atmosenv.2012.02.061, 2012.

Fu, P. Q., Kawamura, K., Chen, J., and Miyazaki, Y.: Secondary Production of Organic Aerosols from Biogenic VOCs over Mt. Fuji, Japan, Environ. Sci. Technol., 48, 8491–8497, https://doi.org/10.1021/es500794d, 2014.

Graham, B., Guyon, P., Taylor, P. E., Artaxo, P., Maenhaut, W., Glovsky, M. M., Flagan, R. C., and Andreae, M. O.: Organic compounds present in the natural Amazonian aerosol: Characterization by gas chromatography–mass spectrometry, J. Geophys. Res-Atmos., 108, https://doi.org/10.1029/2003JD003990, 2003.

Guenther, A., Hewitt, C. N., Erickson, D., Fall, R., Geron, C., Graedel, T., Harley, P., Klinger, L., Lerdau, M., Mckay, W. A., Pierce, T., Scholes, B., Steinbrecher, R., Tallamraju, R., Taylor, J., and Zimmerman, P.: A global model of natural volatile organic compound emissions, Res-Atmos., 100, 8873–8892, https://doi.org/10.1029/94JD02950, 1995.

https://doi.org/10.5194/egusphere-2024-3793
Preprint. Discussion started: 6 January 2025

Guo, S., Hu, M., Guo, Q., Zhang, X., Zheng, M., Zheng, J., Chang, C. C., Schauer, J. J., and Zhang, R.: Primary Sources and Secondary Formation of Organic Aerosols in Beijing, China, Environ. Sci. Technol., 46, 9846–9853, 10.1021/es2042564, 2012.

Guo, W., Li, Z. C., Zhang, Z. Y., Zhu, R. G., Xiao, H. W., and Xiao, H. Y.: Sources and influences of atmospheric nonpolar organic compounds in Nanchang, central China: Full-year monitoring with a focus on winter pollution episodes, Sci. Total Environ., 912, 169216, https://doi.org/10.1016/j.scitotenv.2023.169216, 2024a.

Guo, W., Zhang, Z. Y., Zhu, R. G., Li, Z. C., Liu, C., Xiao, H. W., and Xiao, H. Y.: Pollution characteristics, sources, and health risks of phthalate esters in ambient air: A daily continuous monitoring study in the central Chinese city of Nanchang, Chemosphere, 353, 141564, https://doi.org/10.1016/j.chemosphere.2024.141564, 2024b.

Hallquist, M., Wenger, J. C., Baltensperger, U., Rudich, Y., Simpson, D., Claeys, M., Dommen, J., Donahue, N. M., George, C., Goldstein, A. H., Hamilton, J. F., Herrmann, H., Hoffmann, T., Iinuma, Y., Jang, M., Jenkin, M. E., Jimenez, J. L., Kiendler-Scharr, A., Maenhaut, W., McFiggans, G., Mentel, T. F., Monod, A., Prévôt, A. S. H., Seinfeld, J. H., Surratt, J. D., Szmigielski, R., and Wildt, J.: The formation, properties and impact of secondary organic aerosol: current and emerging issues, Atmos. Chem. Phys., 9, 5155–5236, 10.5194/acp-9-5155-2009, 2009.

Haque, M. M., Kawamura, K., Deshmukh, D. K., Fang, C., Song, W., Mengying, B., and Zhang, Y. L.: Characterization of organic aerosols from a Chinese megacity during winter: predominance of fossil fuel combustion, Atmos. Chem. Phys., 19, 5147–5164, 10.5194/acp-19-5147-2019, 2019.

Haque, M. M., Zhang, Y., Bikkina, S., Lee, M., and Kawamura, K.: Regional heterogeneities in the emission of airborne primary sugar compounds and biogenic secondary organic aerosols in the East Asian outflow: evidence for coal combustion as a source of levoglucosan, Atmos. Chem. Phys., 22, 1373–1393, 10.5194/acp-22-1373-2022, 2022.

Haque, M. M., Verma, S. K., Deshmukh, D. K., Kunwar, B., and Kawamura, K.: Seasonal characteristics of biogenic secondary organic aerosol tracers in a deciduous broadleaf forest in northern Japan, Chemosphere, 311, 136785, https://doi.org/10.1016/j.chemosphere.2022.136785, 2023.

He, L. Y., Hu, M., Huang, X. F., Yu, B. D., Zhang, Y. H., and Liu, D. Q.: Measurement of emissions of fine particulate organic matter from Chinese cooking, Atmos. Environ., 38, 6557–6564, https://doi.org/10.1016/j.atmosenv.2004.08.034, 2004.

https://doi.org/10.5194/egusphere-2024-3793
Preprint. Discussion started: 6 January 2025

Helmig, D., Ortega, J., Guenther, A., Herrick, J. D., and Geron, C.: Sesquiterpene emissions from loblolly pine and their potential contribution to biogenic aerosol formation in the Southeastern US, Atmos. Environ., 40, 4150–4157, https://doi.org/10.1016/j.atmosenv.2006.02.035, 2006.

Hoyle, C. R., Boy, M., Donahue, N. M., Fry, J. L., Glasius, M., Guenther, A., Hallar, A. G., Huff Hartz, K., Petters, M. D., Petäjä, T., Rosenoern, T., and Sullivan, A. P.: A review of the anthropogenic influence on biogenic secondary organic aerosol, Atmos. Chem. Phys., 11, 321–343, https://doi.org/10.5194/acp-11-321-2011, 2011.

Huang, R. J., Zhang, Y., Bozzetti, C., Ho, K. F., Cao, J. J., Han, Y., Daellenbach, K. R., Slowik, J. G., Platt, S. M., Canonaco, F., Zotter, P., Wolf, R., Pieber, S. M., Bruns, E. A., Crippa, M., Ciarelli, G., Piazzalunga, A., Schwikowski, M., Abbaszade, G., Schnelle-Kreis, J., Zimmermann, R., An, Z., Szidat, S., Baltensperger, U., El Haddad, I., and Prevot, A. S.: High secondary aerosol contribution to particulate pollution during haze events in China, Nature, 514, 218–222, https://doi.org/10.1038/nature13774, 2014.

Huebert, B., Bates, T., Russell, P., Shi, G., Kim, Y., Kawamura, K., Carmichael, G., and Nakajima, T.: An overview of ACE-Asia: Strategies for quantifying the relationships between Asian aerosols and their climatic impacts, J. Geophys. Res-Atmos., https://doi.org/108, 10.1029/2003JD003550, 2003.

Iinuma, Y., Brüggemann, E., Gnauk, T., Müller, K., Andreae, M. O., Helas, G., Parmar, R., and Herrmann, H.: Source characterization of biomass burning particles: The combustion of selected European conifers, African hardwood, savanna grass, and German and Indonesian peat, J. Geophys. Res-Atmos., 112, https://doi.org/10.1029/2006JD007120, 2007.

Iyer, S., Rissanen, M. P., Valiev, R., Barua, S., Krechmer, J. E., Thornton, J., Ehn, M., and Kurtén, T.: Molecular mechanism for rapid autoxidation in α-pinene ozonolysis, Nat. Commun., 12, 878, 10.1038/s41467-021-21172-w, 2021.

Jaoui, M., Kleindienst, T. E., Lewandowski, M., Offenberg, J. H., and Edney, E. O.: Identification and Quantification of Aerosol Polar Oxygenated Compounds Bearing Carboxylic or Hydroxyl Groups. 2. Organic Tracer Compounds from Monoterpenes, Environ. Sci. Technol., 39, 5661–5673, 10.1021/es048111b, 2005.

Jaoui, M., Szmigielski, R., Nestorowicz, K., Kolodziejczyk, A., Sarang, K., Rudzinski, K. J., Konopka, A., Bulska, E., Lewandowski, M., and Kleindienst, T. E.: Organic Hydroxy Acids as Highly Oxygenated Molecular (HOM) Tracers for Aged Isoprene Aerosol, Environ. Sci. Technol., 53, 14516–14527, 10.1021/acs.est.9b05075, 2019.

Kanakidou, M., Seinfeld, J. H., Pandis, S. N., Barnes, I., Dentener, F. J., Facchini, M. C., Van Dingenen, R., Ervens, B., Nenes, A., Nielsen, C. J., Swietlicki, E., Putaud, J. P., Balkanski, Y., Fuzzi, S., Horth, J.,

https://doi.org/10.5194/egusphere-2024-3793
Preprint. Discussion started: 6 January 2025

690 Moortgat, G. K., Winterhalter, R., Myhre, C. E. L., Tsigaridis, K., Vignati, E., Stephanou, E. G., and
691 Wilson, J.: Organic aerosol and global climate modelling: a review, Atmos. Chem. Phys., 5, 1053–1123,
692 https://doi.org/10.5194/acp-5-1053-2005, 2005.
693 Kawamura, K., and Gagosian, R. B.: Implications of ω-oxocarboxylic acids in the remote marine atmosphere
694 for photo-oxidation of unsaturated fatty acids, Nature, 325, 330–332, https://doi.org/10.1038/325330a0,
695 1987.
696 Kawamura, K., and Kaplan, I. R.: Motor exhaust emissions as a primary source for dicarboxylic acids in Los
697 Angeles ambient air, Environ. Sci. Technol., 21, 105–110, https://doi.org/10.1021/es00155a014, 1987.
698 Kawamura, K., and Ikushima, K.: Seasonal changes in the distribution of dicarboxylic acids in the urban
699 atmosphere, Environ. Sci. Technol., 27, 2227–2235, https://doi.org/10.1021/ES00047A033, 1993.
700 Kawamura, K., and Sakaguchi, F.: Molecular distributions of water soluble dicarboxylic acids in marine
701 aerosols over the Pacific Ocean including tropics, J. Geophys. Res-Atmos., 104, 3501–3509,
702 https://doi.org/10.1029/1998JD100041, 1999.
703 Kawamura, K., Steinberg, S., and Kaplan, I. R.: Homologous series of C1–C10 monocarboxylic acids and C1–
704 C6 carbonyls in Los Angeles air and motor vehicle exhausts, Atmos. Environ., 34, 4175–4191,
705 https://doi.org/10.1016/S1352-2310(00)00212-0, 2000.
706 Kawamura, K., Ishimura, Y., and Yamazaki, K.: Four years' observations of terrestrial lipid class compounds
707 in marine aerosols from the western North Pacific, Global Biogeochem. Cy., 17, 1003,
708 https://doi.org/10.1029/2001GB001810, 2003.
709 Kleindienst, T. E., Jaoui, M., Lewandowski, M., Offenberg, J. H., Lewis, C. W., Bhave, P. V., and Edney, E.
710 O.: Estimates of the contributions of biogenic and anthropogenic hydrocarbons to secondary organic
711 aerosol at a southeastern US location, Atmos. Environ., 41, 8288–8300,
712 https://doi.org/10.1016/j.atmosenv.2007.06.045, 2007.
713 Kleindienst, T. E., Lewandowski, M., Offenberg, J. H., Jaoui, M., and Edney, E. O.: The formation of
714 secondary organic aerosol from the isoprene $^{+}$OH reaction in the absence of NO_x, Atmos. Chem. Phys., 9,
715 6541–6558, 10.5194/acp-9-6541-2009, 2009.
716 Kleindienst, T.E., Jaoui, M., Lewandowski, M., Offenberg, J.H., and Docherty, K.S.: The formation of SOA
717 and chemical tracer compounds from the photooxidation of naphthalene and its methyl analogs in the
718 presence and absence of nitrogen oxides, Atmos. Chem. Phys., 12, 8711–8726 https://doi.org/10.5194/acp-
719 12-8711-2012, 2012.

https://doi.org/10.5194/egusphere-2024-3793
Preprint. Discussion started: 6 January 2025

720 Kunwar, B., and Kawamura, K.: One-year observations of carbonaceous and nitrogenous components and
721 major ions in the aerosols from subtropical Okinawa Island, an outflow region of Asian dusts, Atmos.
722 Chem. Phys., 14, 1819–1836, https://doi.org/10.5194/acp-14-1819-2014, 2014.
723 Lewandowski, M., Jaoui, M., Offenberg, J. H., Kleindienst, T. E., Edney, E. O., Sheesley, R. J., and Schauer, J.
724 J.: Primary and secondary contributions to ambient PM in the midwestern United States, Environ. Sci.
725 Technol., 42, 3303–3309, https://doi.org/doi: 10.1021/es0720412, 2008.
726 Lewandowski, M., Piletic, I. R., Kleindienst, T. E., Offenberg, J. H., Beaver, M. R., Jaoui, M., Docherty, K. S.,
727 and Edney, E. O.: Secondary organic aerosol characterisation at field sites across the United States during
728 the spring–summer period, Int. J. Environ. An. Ch., 93, 1084–1103,
729 https://doi.org/10.1080/03067319.2013.803545, 2013.
730 Li, J. J., Wang, G. H., Wu, C., Cao, C., Ren, Y.Q., Wang, J. Y., Li, J., Cao, J. J., Zeng, L. M., and Zhu, T.:
731 Characterization of isoprene-derived secondary organic aerosols at a rural site in North China Plain with
732 implications for anthropogenic pollution effects, Sci. Rep-Uk., 8, 535, https://doi.org/10.1038/s41598-017-
733 18983-7, 2018.
734 Li, J. J., Wang, G. H., Zhang, Q., Li, J., Wu, C., Jiang, W. Q., Zhu, T., and Zeng, L. M.: Molecular
735 characteristics and diurnal variations of organic aerosols at a rural site in the North China Plain with
736 implications for the influence of regional biomass burning, Atmos. Chem. Phys., 19, 10481–
737 https://doi.org/10496, 10.5194/acp-19-10481-2019, 2019.
738 Lin, Y. H., Zhang, Z., Docherty, K. S., Zhang, H., Budisulistiorini, S. H., Rubitschun, C. L., Shaw, S. L.,
739 Knipping, E. M., Edgerton, E. S., Kleindienst, T. E., Gold, A., and Surratt, J. D.: Isoprene Epoxydiols as
740 Precursors to Secondary Organic Aerosol Formation: Acid-Catalyzed Reactive Uptake Studies with
741 Authentic Compounds, Environ. Sci. Technol., 46, 250–258, https://doi.org/10.1021/es202554c, 2012.
742 Lin, Y. H., Knipping, E. M., Edgerton, E. S., Shaw, S. L., and Surratt, J. D.: Investigating the influences of
743 SO_2 and NH_3 levels on isoprene-derived secondary organic aerosol formation using conditional sampling
744 approaches, Atmos. Chem. Phys., 13, 8457–8470, https://doi.org/10.5194/acp-13-8457-2013, 2013.
745 Ng, N. L., Brown, S. S., Archibald, A. T., Atlas, E., Cohen, R. C., Crowley, J. N., Day, D. A., Donahue, N. M.,
746 Fry, J. L., Fuchs, H., Griffin, R. J., Guzman, M. I., Herrmann, H., Hodzic, A., Iinuma, Y., Jimenez, J. L.,
747 Kiendler-Scharr, A., Lee, B. H., Luecken, D. J., Mao, J., McLaren, R., Mutzel, A., Osthoff, H. D., Ouyang,
748 B., Picquet-Varrault, B., Platt, U., Pye, H. O. T., Rudich, Y., Schwantes, R. H., Shiraiwa, M., Stutz, J.,
749 Thornton, J. A., Tilgner, A., Williams, B. J., and Zaveri, R. A.: Nitrate radicals and biogenic volatile
750 organic compounds: oxidation, mechanisms, and organic aerosol, Atmos. Chem. Phys., 17, 2103–2162,
751 https://doi.org/10.5194/acp-17-2103-2017, 2017.

https://doi.org/10.5194/egusphere-2024-3793
Preprint. Discussion started: 6 January 2025

752 Nguyen, T. B., Bates, K. H., Crounse, J. D., Schwantes, R. H., Zhang, X., Kjaergaard, H. G., Surratt, J. D., Lin,
753 P., Laskin, A., Seinfeld, J. H., and Wennberg, P. O.: Mechanism of the hydroxyl radical oxidation of
754 methacryloyl peroxynitrate (MPAN) and its pathway toward secondary organic aerosol formation in the
755 atmosphere, Chem. Phys., 17, 17914–17926, https://doi.org/10.1039/c5cp02001h, 2015.
756 Nolte, C. G., Schauer, J. J., Cass, G. R., and Simoneit, B. R. T.: Highly Polar Organic Compounds Present in
757 Meat Smoke, Environ. Sci. Technol., 33, 3313–3316, https://doi.org/10.1021/es990122v, 1999.
758 Nolte, C. G., Schauer, J. J., Cass, G. R., and Simoneit, B. R. T.: Highly Polar Organic Compounds Present in
759 Wood Smoke and in the Ambient Atmosphere, Environ. Sci. Technol., 35, 1912–1919,
760 https://doi.org/10.1021/es001420r, 2001.
761 Nozière, B., González, N. J. D., Borg-Karlson, A. K., Pei, Y. X., Redeby, J. P., Krejci, R., Dommen, J., Prévôt,
762 A. S. H., and Anthonsen, T.: Atmospheric chemistry in stereo: A new look at secondary organic aerosols
763 from isoprene, Geophys. Res. Lett., 38, https://doi.org/10.1029/2011GL047323 , 2011.
764 Oros, D. R., and Simoneit, B. R. T.: Identification and emission rates of molecular tracers in coal smoke
765 particulate matter, Fuel, 79, 515–536, https://doi.org/10.1016/S0016-2361(99)00153-2, 2000.
766 Oros, D. R., and Simoneit, B. R. T.: Identification and emission factors of molecular tracers in organic aerosols
767 from biomass burning Part 2. Deciduous trees, Appl. Geochem., 16, 1545–1565,
768 https://doi.org/10.1016/S0883-2927(01)00022-1, 2001.
769 Piccot, S. D., Watson, J. J., and Jones, J. W.: A global inventory of volatile organic compound emissions from
770 anthropogenic sources, J. Geophys. Res., 97, 9897–9912, https://doi.org/10.1029/92JD00682, 1992.
771 Puxbaum, H., and Tenze-Kunit, M.: Size distribution and seasonal variation of atmospheric cellulose, Atmos.
772 Environ., 37, 3693–3699, https://doi.org/10.1016/S1352-2310(03)00451-5, 2003.
773 Ren, H., Hu, W., Wei, L. F., Yue, S. Y., Zhao, J., Li, L. J., Wu, L. B., Zhao, W. Y., Ren, L. J., Kang, M. J., Xie,
774 Q. Y., Su, S. H., Pan, X. L., Wang, Z. F., Sun, Y. L., Kawamura, K., and Fu, P. Q.: Measurement report:
775 Vertical distribution of biogenic and anthropogenic secondary organic aerosols in the urban boundary layer
776 over Beijing during late summer, Atmos. Chem. Phys., 21, 12949–12963, https://doi.org/10.5194/acp-21-
777 12949-2021, 2021.
778 Ren, Y. Q., Wang, G. H., Tao, J., Zhang, Z. S., Wu, C., Wang, J. Y., Li, J. J, Wei, J., Li, H., and Meng, F.:
779 Seasonal characteristics of biogenic secondary organic aerosols at Mt. Wuyi in Southeastern China:
780 Influence of anthropogenic pollutants, Environ. Pollut., 252, 493–500,
781 https://doi.org/10.1016/j.envpol.2019.05.077, 2019.

https://doi.org/10.5194/egusphere-2024-3793
Preprint. Discussion started: 6 January 2025

Riipinen, I., Yli-Juuti, T., Pierce, J. R., Petaja, T., Worsnop, D. R., Kulmala, M., and Donahue, N. M.: The contribution of organics to atmospheric nanoparticle growth, Nat. Geosci., 5, 453–458, https://doi.org/10.1038/ngeo1499, 2012.

Rogge, W. F., Hildemann, L. M., Mazurek, M. A., Cass, G. R., and Simoneit, B. R. T.: Sources of fine organic aerosol. 1. Charbroilers and meat cooking operations, Environ. Sci. Technol., 25, 1112–1125, https://doi.org/10.1021/es00018a015, 1991.

Rogge, W. F., Hildemann, L. M., Mazurek, M. A., Cass, G. R., Simoneit, B. R. T. J. E. S., and Technology: Sources of fine organic aerosol. 2. Noncatalyst and catalyst-equipped automobiles and heavy-duty diesel trucks, Environ. Sci. Technol., 27, 636–651, https://doi.org/10.1021/es00041a007, 1993.

Rogge, W. F., Medeiros, P. M., and Simoneit, B. R. T.: Organic marker compounds for surface soil and fugitive dust from open lot dairies and cattle feedlots, Atmos. Environ., 40, 27–49, https://doi.org/10.1016/j.atmosenv.2005.07.076, 2006.

Rudich, Y., Donahue, N. M., and Mentel, T. F.: Aging of organic aerosol: bridging the gap between laboratory and field studies, Annu. Rev. Phys. Chem., 58, 321–352, https://doi.org/10.1146/annurev.physchem.58.032806.104432, 2007.

Rybicki, M., Marynowski, L., Bechtel, A., and Simoneit, B. R. T.: Variations in δ13C values of levoglucosan from low-temperature burning of lignite and biomass, Sci. Total Environ., 733, 138991, https://doi.org/10.1016/j.scitotenv.2020.138991, 2020a.

Rybicki, M., Marynowski, L., and Simoneit, B. R. T.: Composition of organic compounds from low-temperature burning of lignite and their application as tracers in ambient air, Chemosphere, 249, 126087, https://doi.org/10.1016/j.chemosphere.2020.126087, 2020b.

Saarikoski, S., Timonen, H., Saarnio, K., Aurela, M., Järvi, L., Keronen, P., Kerminen, V. M., and Hillamo, R.: Sources of organic carbon in fine particulate matter in northern European urban air, Atmos. Chem. Phys., 8, 6281–6295, https://doi.org/10.5194/acp-8-6281-2008, 2008.

Sharkey, T. D., Wiberley, A. E., and Donohue, A. R.: Isoprene emission from plants: why and how, Annals of botany, 101, 5–18, https://doi.org/10.1093/aob/mcm240, 2008.

Sheesley, R. J., Schauer, J. J., Chowdhury, Z., Cass, G. R., and Simoneit, B. R. T.: Characterization of organic aerosols emitted from the combustion of biomass indigenous to South Asia, J. Geophys. Res-Atmos., 108, https://doi.org/10.1029/2002JD002981, 2003.

Shiraiwa, M., Ueda, K., Pozzer, A., Lammel, G., Kampf, C. J., Fushimi, A., Enami, S., Arangio, A. M., Fröhlich-Nowoisky, J., Fujitani, Y., Furuyama, A., Lakey, P. S. J., Lelieveld, J., Lucas, K., Morino, Y., Pöschl, U., Takahama, S., Takami, A., Tong, H., Weber, B., Yoshino, A., and Sato, K.: Aerosol Health

https://doi.org/10.5194/egusphere-2024-3793
Preprint. Discussion started: 6 January 2025

814 Effects from Molecular to Global Scales, Environ. Sci. Technol., 51, 13545–13567,
815 10.1021/acs.est.7b04417, 2017.
816 Simoneit, B. R. T.: Biomass burning — a review of organic tracers for smoke from incomplete combustion,
817 Applied Geochemistry, 17, 129–162, https://doi.org/10.1016/S0883-2927(01)00061-0, 2002.
818 Simoneit, B. R. T., Kobayashi, M., Mochida, M., Kawamura, K., and Huebert, B. J.: Aerosol particles
819 collected on aircraft flights over the northwestern Pacific region during the ACE-Asia campaign:
820 Composition and major sources of the organic compounds, J. Geophys. Res-Atmos., 109,
821 https://doi.org/10.1029/2004JD004565, 2004a.
822 Simoneit, B. R., Elias, V. O., Kobayashi, M., Kawamura, K., Rushdi, A. I., Medeiros, P. M., Rogge, W. F.,
823 and Didyk, B. M.: Sugars-dominant water-soluble organic compounds in soils and characterization as
824 tracers in atmospheric particulate matter, Environ. Sci. Technol., 38, 5939–5949,
825 https://doi.org/10.1021/es0403099, 2004b.
826 Srivastava, D., Vu, T. V., Tong, S., Shi, Z., and Harrison, R. M.: Formation of secondary organic aerosols
827 from anthropogenic precursors in laboratory studies, Npj. Clim. Atmos. Sci., 5, 22,
828 https://doi.org/10.1038/s41612-022-00238-6, 2022.
829 Stohl, A., Berg, T., Burkhart, J. F., Fjæraa, A. M., Forster, C., Herber, A., Hov, Ø., Lunder, C., McMillan, W.
830 W., Oltmans, S., Shiobara, M., Simpson, D., Solberg, S., Stebel, K., Ström, J., Tørseth, K., Treffeisen, R.,
831 Virkkunen, K., and Yttri, K. E.: Arctic smoke – record high air pollution levels in the European
832 Arctic due to agricultural fires in Eastern Europe in spring 2006, Atmos. Chem. Phys., 7, 511–534,
833 https://doi.org/10.5194/acp-7-511-2007, 2007.
834 Stone, E. A., Zhou, J., Snyder, D. C., Rutter, A. P., Mieritz, M., and Schauer, J. J.: A comparison of
835 summertime secondary organic aerosol source contributions at contrasting urban locations, Environ. Sci.
836 Technol., 43, 3448–3454, https://doi.org/10.1021/es8025209, 2009.
837 Surratt, J. D., Murphy, S. M., Kroll, J. H., Ng, N. L., Hildebrandt, L., Sorooshian, A., Szmigielski, R.,
838 Vermeylen, R., Maenhaut, W., Claeys, M., Flagan, R. C., and Seinfeld, J. H.: Chemical Composition of
839 Secondary Organic Aerosol Formed from the Photooxidation of Isoprene, J. Phys. Chem. A, 110, 9665–
840 9690, 10.1021/jp061734m, 2006.
841 Surratt, J. D., Chan, A. W. H., Eddingsaas, N. C., Chan, M., Loza, C. L., Kwan, A. J., Hersey, S. P., Flagan, R.
842 C., Wennberg, P. O., and Seinfeld, J. H.: Reactive intermediates revealed in secondary organic aerosol
843 formation from isoprene, Proc. Natl. Acad. Sci. U.S.A., 107, 6640–6645,
844 https://doi.org/doi:10.1073/pnas.0911114107, 2010.

https://doi.org/10.5194/egusphere-2024-3793
Preprint. Discussion started: 6 January 2025

845 Tang, T. G., Cheng, Z. N., Xu, B. Q., Zhang, B. L., Li, J., Zhang, W., Wang, K. L., and Zhang, G.: Source
846 Diversity of Intermediate Volatility n-Alkanes Revealed by Compound-Specific $\delta^{13}C-\delta D$ Isotopes, Environ.
847 Sci. Technol., 56, 14262–14271, 10.1021/acs.est.2c02156, 2022.
848 Turpin, B. J., and Huntzicker, J. J.: Identification of secondary organic aerosol episodes and quantitation of
849 primary and secondary organic aerosol concentrations during SCAQS, Atmos. Environ., 29, 3527–3544,
850 https://doi.org/10.1016/1352-2310(94)00276-Q, 1995.
851 von Schneidemesser, E., Zhou, J., Stone, E. A., Schauer, J. J., Shpund, J., Brenner, S., Qasrawi, R., Abdeen, Z.,
852 and Sarnat, J. A.: Spatial Variability of Carbonaceous Aerosol Concentrations in East and West Jerusalem,
853 Environ. Sci. Technol., 44, 1911–1917, https://doi.org/10.1021/es9014025, 2010.
854 Wang, G. H., and Kawamura, K.: Molecular Characteristics of Urban Organic Aerosols from Nanjing: A Case
855 Study of A Mega-City in China, Environ. Sci. Technol., 39, 7430–7438, https://doi.org/10.1021/es051055,
856 2005.
857 Wang, G. H., Kawamura, K., Lee, S., Ho, K., and Cao, J. J.: Molecular, Seasonal, and Spatial Distributions of
858 Organic Aerosols from Fourteen Chinese Cities, Environ. Sci. Technol., 40, 4619–4625,
859 https://doi.org/10.1021/es060291x, 2006.
860 Wang, G. H., Kawamura, K., Hatakeyama, S., Takami, A., Li, H., and Wang, W.: Aircraft Measurement of
861 Organic Aerosols over China, Environ. Sci. Technol., 41, 3115–3120, https://doi.org/10.1021/es062601h,
862 2007.
863 Weber, R. J., Sullivan, A. P., Peltier, R. E., Russell, A. G., Yan, B., Zheng, M., Gouw, J. d., Warneke, C.,
864 Brock, C. A., Holloway, J. S., Atlas, E. L., and Edgerton, E. S.: A study of secondary organic aerosol
865 formation in the anthropogenic-influenced southeastern United States, J. Geophys. Res-Atmos., 112,
866 https://doi.org/10.1029/2007JD008408, 2007.
867 Wu, J. R., Bei, N. F., Wang, Y., Li, X., Liu, S. X., Liu, L., Wang, R. N., Yu, J. Y., Le, T. H., Zuo, M., Shen, Z.
868 X., Cao, J. J., Tie, X. X., and Li, G. H.: Insights into particulate matter pollution in the North China Plain
869 during wintertime: local contribution or regional transport?, Atmos. Chem. Phys., 21, 2229–2249,
870 https://doi.org/10.5194/acp-21-2229-2021, 2021.
871 Xu, B. Q., Tang, J., Tang, T. G., Zhao, S. Z., Zhong, G. C., Zhu, S. Y., Li, J., and Zhang, G.: Fates of
872 secondary organic aerosols in the atmosphere identified from compound-specific dual-carbon isotope
873 analysis of oxalic acid, Atmos. Chem. Phys., 23, 1565–1578, https://doi.org/10.5194/acp-23-1565-2023,
874 2023.
875 Xu, B. Q., Zhang, G., Gustafsson, Ö., Kawamura, K., Li, J., Andersson, A., Bikkina, S., Kunwar, B., Pokhrel,
876 A., Zhong, G. C., Zhao, S. Z., Li, J., Huang, C., Cheng, Z. N., Zhu, S. Y., Peng, P. A., and Sheng, G. Y.:

https://doi.org/10.5194/egusphere-2024-3793
Preprint. Discussion started: 6 January 2025

Large contribution of fossil-derived components to aqueous secondary organic aerosols in China, Nat. Commun., 13, 5115, https://doi.org/10.1038/s41467-022-32863-3, 2022.

Xu, J. S., Liu, D., Wu, X. F., Vu, T. V., Zhang, Y. L., Fu, P. Q., Sun, Y. L., Xu, W. Q., Zheng, B., Harrison, R. M., and Shi, Z. B.: Source apportionment of fine organic carbon at an urban site of Beijing using a chemical mass balance model, Atmos. Chem. Phys., 21, 7321–7341, https://doi.org/10.5194/acp-21-7321-2021, 2021.

Yan, C. C., Sullivan, A. P., Cheng, Y., Zheng, M., Zhang, Y. H., Zhu, T., and Collett, J. L.: Characterization of saccharides and associated usage in determining biogenic and biomass burning aerosols in atmospheric fine particulate matter in the North China Plain, Sci. Total Environ., 650, 2939–2950, https://doi.org/10.1016/j.scitotenv.2018.09.325, 2019.

Yazdani, A., Dudani, N., Takahama, S., Bertrand, A., Prévôt, A. S. H., El Haddad, I., and Dillner, A. M.: Characterization of primary and aged wood burning and coal combustion organic aerosols in an environmental chamber and its implications for atmospheric aerosols, Atmos. Chem. Phys., 21, 10273–10293, https://doi.org/10.5194/acp-21-10273-2021, 2021.

Yee, L. D., Isaacman-VanWertz, G., Wernis, R. A., Kreisberg, N. M., Glasius, M., Riva, M., Surratt, J. D., de Sá, S. S., Martin, S. T., Alexander, M. L., Palm, B. B., Hu, W., Campuzano-Jost, P., Day, D. A., Jimenez, J. L., Liu, Y., Misztal, P. K., Artaxo, P., Viegas, J., Manzi, A., de Souza, R. A. F., Edgerton, E. S., Baumann, K., and Goldstein, A. H.: Natural and Anthropogenically Influenced Isoprene Oxidation in Southeastern United States and Central Amazon, Environ. Sci. Technol., 54, 5980–5991, https://doi.org/10.1021/acs.est.0c00805, 2020.

Yttri, K. E., Dye, C., and Kiss, G.: Ambient aerosol concentrations of sugars and sugar-alcohols at four different sites in Norway, Atmos. Chem. Phys., 7, 4267–4279, https://doi.org/10.5194/acp-7-4267-2007, 2007.

Zhang, Q., He, K. B., and Huo, H.: Cleaning China's air, Nature, 484, 161–162, https://doi.org/10.1038/484161a, 2012.

Zhang, Q., Hu, W., Ren, H., Yang, J. B., Deng, J. J., Wang, D. W., Sun, Y. L., Wang, Z. F., Kawamura, K., and Fu, P. Q.: Diurnal variations in primary and secondary organic aerosols in an eastern China coastal city: The impact of land-sea breezes, Environ. Pollut., 319, 121016, https://doi.org/10.1016/j.envpol.2023.121016, 2023.

Zhang, X., McVay, R. C., Huang, D. D., Dalleska, N. F., Aumont, B., Flagan, R. C., and Seinfeld, J. H.: Formation and evolution of molecular products in α-pinene secondary organic aerosol, Proc. Natl. Acad. Sci. U. S. A., 112, 14168–14173, https://doi.org/10.1073/pnas.1517742112, 2015.

https://doi.org/10.5194/egusphere-2024-3793
Preprint. Discussion started: 6 January 2025

909 Zhang, Y. X., Cao, F., Song, W. H., Jia, X. F., Xie, T., Wu, C.L., Yan, P., Yu, M. Y., Rauber, M., Salazar, G.,
910 Szidat, S., and Zhang, Y. L.: Fossil and Nonfossil Sources of Winter Organic Aerosols in the Regional
911 Background Atmosphere of China, Environ. Sci. Technol., 58, 1244–1254,
912 https://doi.org/10.1021/acs.est.3c08491, 2024.
913 Zhang, Y. X., Schauer, J. J., Zhang, Y. H., Zeng, L. M., Wei, Y. J., Liu, Y., and Shao, M.: Characteristics of
914 Particulate Carbon Emissions from Real-World Chinese Coal Combustion, Environ. Sci. Technol., 42,
915 5068–5073, https://doi.org/10.1021/es7022576, 2008.
916 Zhang, Y. L., Kawamura, K., Agrios, K., Lee, M., Salazar, G., and Szidat, S.: Fossil and Nonfossil Sources of
917 Organic and Elemental Carbon Aerosols in the Outflow from Northeast China, Environ. Sci. Technol., 50,
918 6284–6292, https://doi.org/10.1021/acs.est.6b00351, 2016.
919 Zhao, Y. L., Hu, M., Slanina, S., and Zhang, Y. H.: Chemical Compositions of Fine Particulate Organic Matter
920 Emitted from Chinese Cooking, Environ. Sci. Technol., 41, 99–105, https://doi.org/10.1021/es0614518,
921 2007.
922 Zhu, C. M., Kawamura, K., and Fu, P. Q.: Seasonal variations of biogenic secondary organic aerosol tracers in
923 Cape Hedo, Okinawa, Atmos. Environ., 130, 113–119, https://doi.org/10.1016/j.atmosenv.2015.08.069,
924 2016.
925 Zhu, R. G., Xiao, H. Y., Cheng, L., Zhu, H., Xiao, H., and Gong, Y. Y.: Measurement report: Characterization
926 of sugars and amino acids in atmospheric fine particulates and their relationship to local primary sources,
927 Atmos. Chem. Phys., 22, 14019–14036, 10.5194/acp-22-14019-2022, 2022.
928
929
930
931
932
933
934
935
936

https://doi.org/10.5194/egusphere-2024-3793
Preprint. Discussion started: 6 January 2025

Figure Captions

Figure 1. (a) Average $PM_{2.5}$ concentrations across various cities in China during winter 2023–2024 (December 2023 to February 2024). (b) Location of sampling sites in Nanchang.

Figure 2. One-year time series of organic carbon (OC), elemental carbon (EC), OC/EC ratios, $PM_{2.5}$ concentrations, and concentrations of polar organic compounds.

Figure 3. Molecular characteristics and seasonal variations of the major polar compounds in $PM_{2.5}$.

Figure 4. The concentration ratios and its seasonal variations of the major polar compounds. Each box plot illustrates the mean (centerline), interquartile range (box encompassing the 25th to 75th percentiles), and standard deviation (whiskers).

Figure 5. Molecular characteristics and seasonal variations of the minor polar compounds in $PM_{2.5}$.

Figure 6. Molecular characteristics and seasonal variations of the SOA tracers in $PM_{2.5}$.

Figure 7. The concentration ratios and its seasonal variations of the SOA tracers. Box plots represent the mean (centerline), interquartile range (box encompassing the 25th to 75th percentiles), and standard deviation (whiskers).

Figure 8. Concentrations and relative abundances of primary organic carbon (POC) from biomass burning (POC_{bb}), coal combustion (POC_{cc}), vehicle exhaust (POC_{ve}), cooking (POC_c), plant debris (POC_{pd}), and fungal spores (POC_{fs}), alongside secondary organic carbon (SOC) from isoprene (SOC_i), α/β-pinene (SOC_p), β-caryophyllene (SOC_c), toluene (SOC_t), and naphthalene (SOC_n). POC and SOC concentrations were estimated by the tracer-based method, and other OC (OOC) was obtained by subtracting estimated OC from measured OC.

Figure 9. Pearson correlation between POC, SOC, and the measured OC during the annual sampling period and winter pollution episodes. Circle size represents the contribution (%) of POC and SOC to the variation in measured OC, as determined by redundancy analysis. Magenta circles represent P-values from correlation and redundancy analyses that are less than 0.05, while gray circles indicate P-values greater than 0.05. Definitions: POC_{bb} (biomass burning), POC_{cc} (coal combustion), POC_{ve} (vehicle exhaust), POC_c (cooking), POC_{pd} (plant debris), POC_{fs} (fungal spores), and $POC_{EC\text{-}based}$ (based on EC method). SOC_i, SOC_p, SOC_c, SOC_t, SOC_n, and

https://doi.org/10.5194/egusphere-2024-3793
Preprint. Discussion started: 6 January 2025

$SOC_{EC\text{-}based}$ refer to SOC from isoprene, α/β-pinene, β-caryophyllene, toluene, naphthalene, and EC-based methods, respectively.

Figure 10. Linear correlation between temperature, NO_2, and SOC during specific winter pollution episode. SOC concentrations were estimated by the tracer-based method.

https://doi.org/10.5194/egusphere-2024-3793
Preprint. Discussion started: 6 January 2025

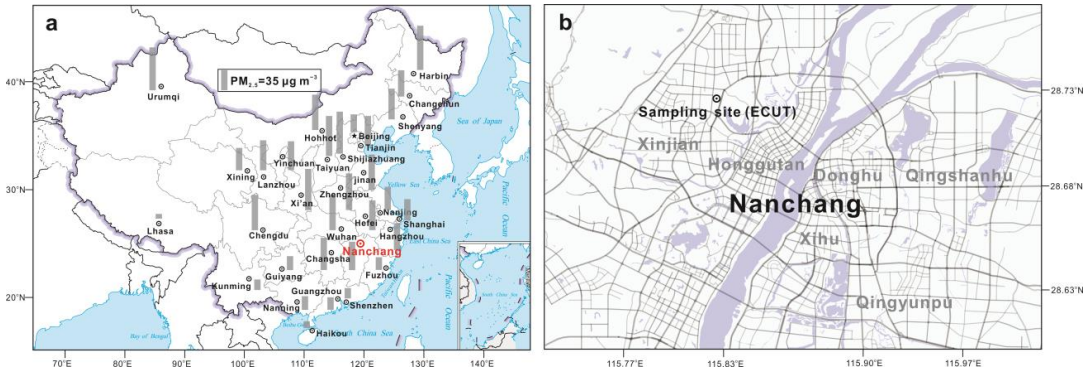

Figure 1. (a) Average $PM_{2.5}$ concentrations across various cities in China during winter 2023–2024 (December 2023 to February 2024). (b) Location of sampling sites in Nanchang.

https://doi.org/10.5194/egusphere-2024-3793
Preprint. Discussion started: 6 January 2025

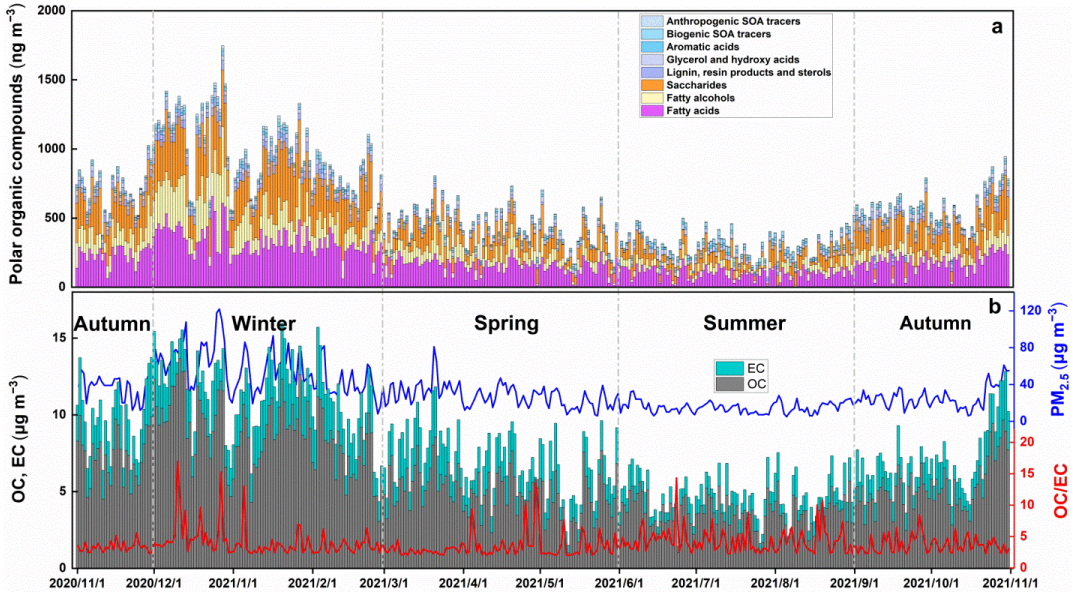

Figure 2. One-year time series of organic carbon (OC), elemental carbon (EC), OC/EC ratios, $PM_{2.5}$ concentrations, and concentrations of polar organic compounds.

https://doi.org/10.5194/egusphere-2024-3793
Preprint. Discussion started: 6 January 2025

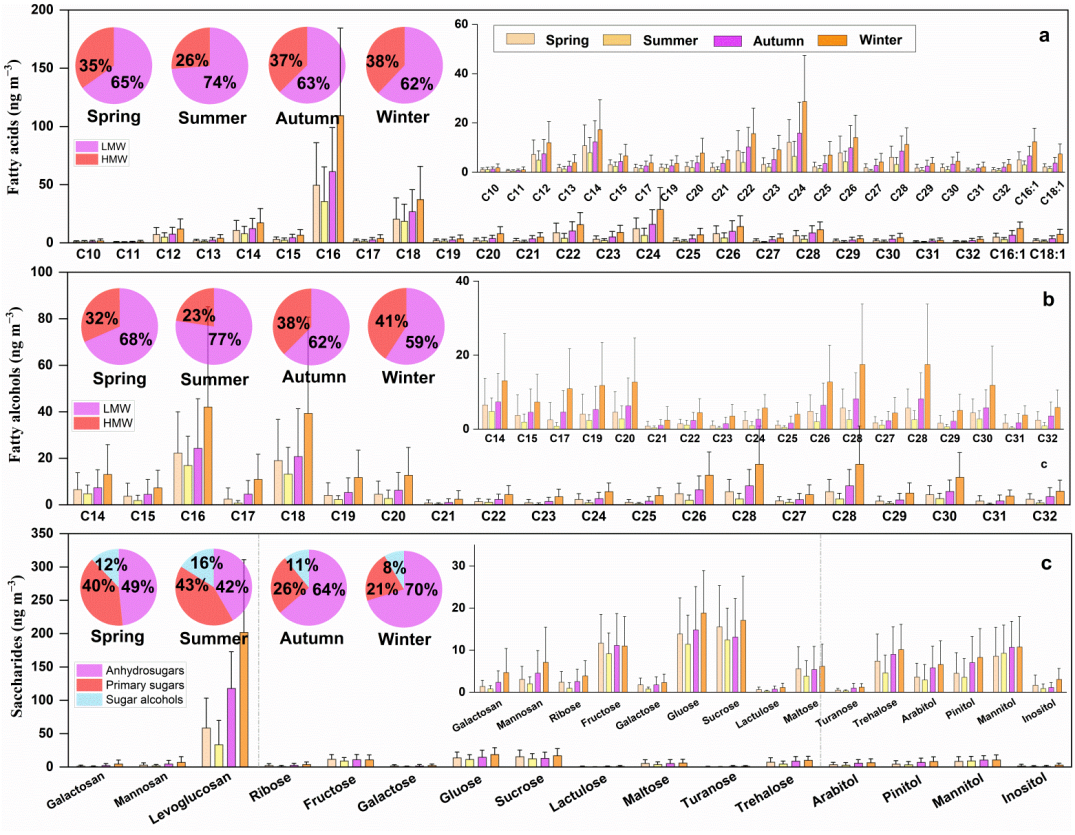

Figure 3. Molecular characteristics and seasonal variations of the major polar compounds in $PM_{2.5}$.

https://doi.org/10.5194/egusphere-2024-3793
Preprint. Discussion started: 6 January 2025

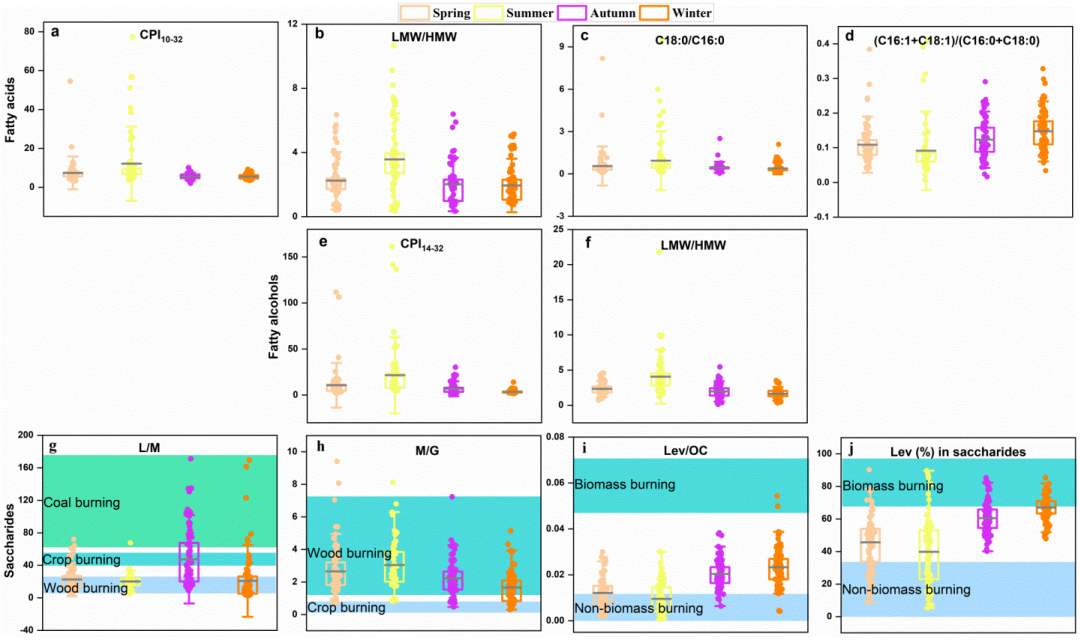

Figure 4. The concentration ratios and its seasonal variations of the major polar compounds. Each box plot illustrates the mean (centerline), interquartile range (box encompassing the 25th to 75th percentiles), and standard deviation (whiskers).

https://doi.org/10.5194/egusphere-2024-3793
Preprint. Discussion started: 6 January 2025

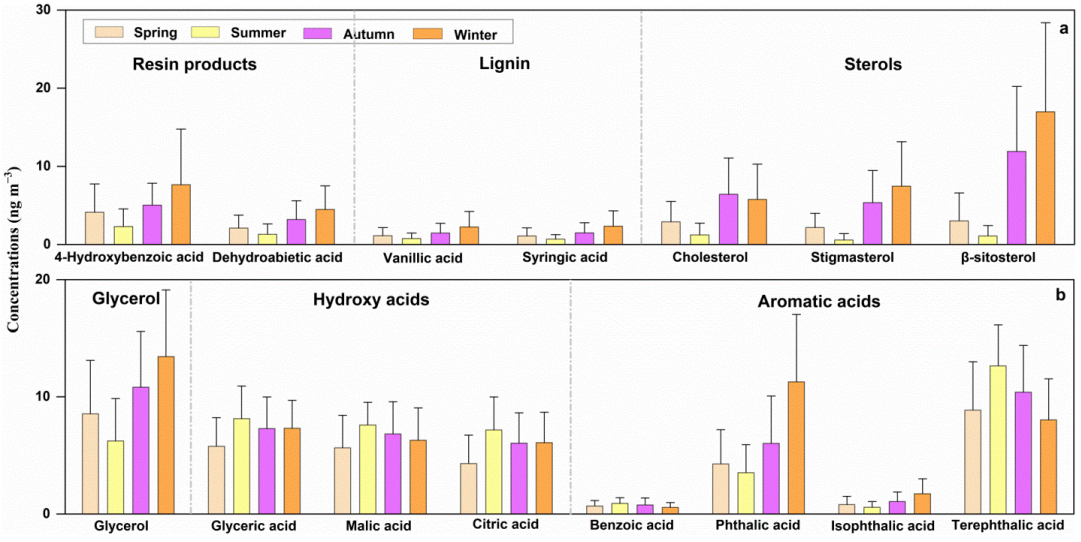

Figure 5. Molecular characteristics and seasonal variations of the minor polar compounds in $PM_{2.5}$.

https://doi.org/10.5194/egusphere-2024-3793
Preprint. Discussion started: 6 January 2025

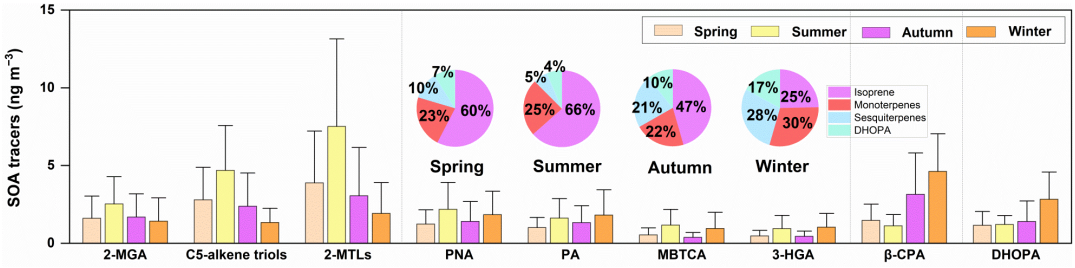

Figure 6. Molecular characteristics and seasonal variations of the SOA tracers in $PM_{2.5}$.

https://doi.org/10.5194/egusphere-2024-3793
Preprint. Discussion started: 6 January 2025

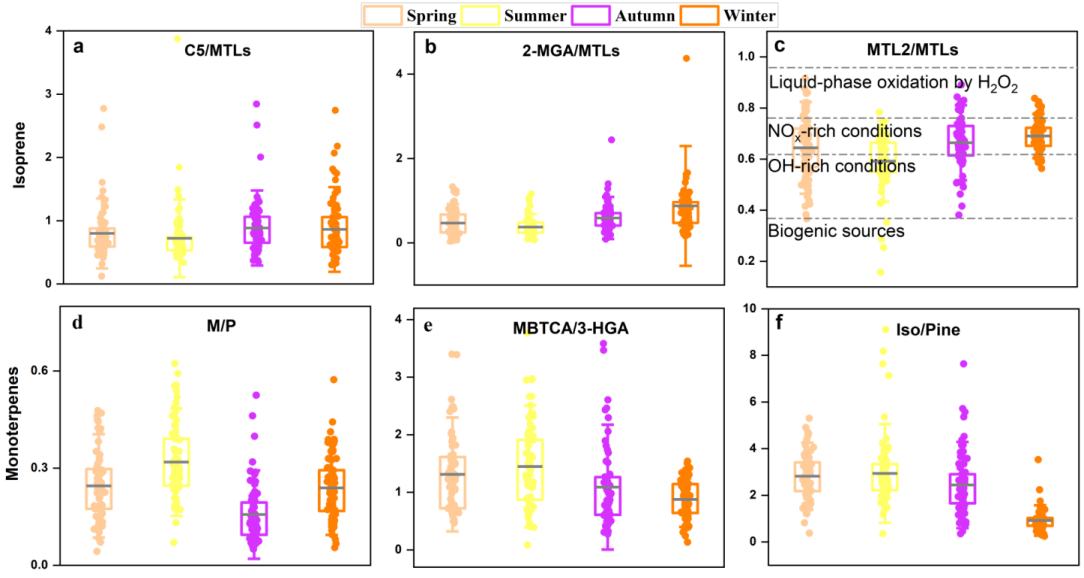

Figure 7. The concentration ratios and its seasonal variations of the SOA tracers. Box plots represent the mean (centerline), interquartile range (box encompassing the 25th to 75th percentiles), and standard deviation (whiskers).

https://doi.org/10.5194/egusphere-2024-3793
Preprint. Discussion started: 6 January 2025

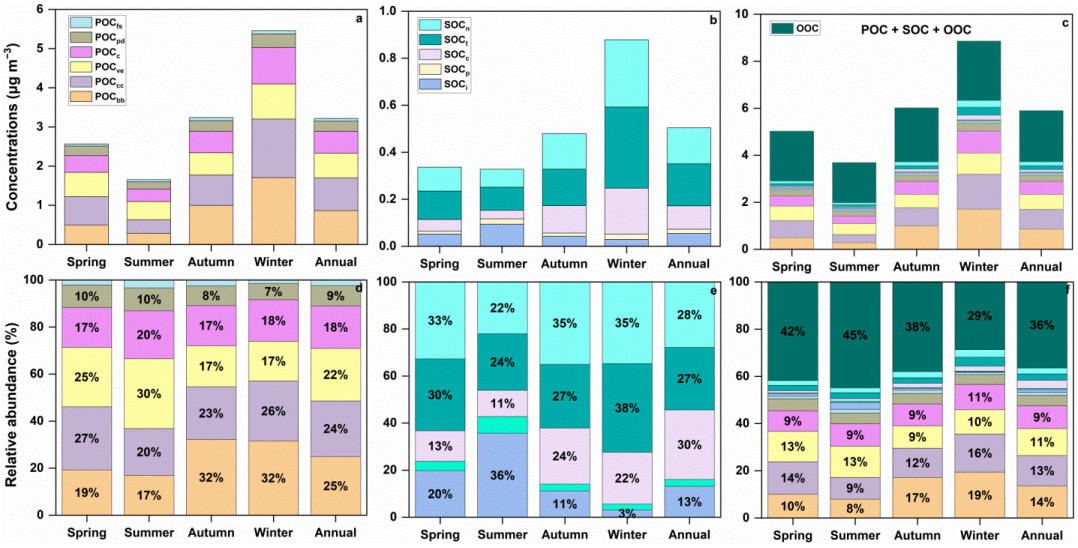

Figure 8. Concentrations and relative abundances of primary organic carbon (POC) from biomass burning (POC_{bb}), coal combustion (POC_{cc}), vehicle exhaust (POC_{ve}), cooking (POC_c), plant debris (POC_{pd}), and fungal spores (POC_{fs}), alongside secondary organic carbon (SOC) from isoprene (SOC_i), α/β-pinene (SOC_p), β-caryophyllene (SOC_c), toluene (SOC_t), and naphthalene (SOC_n). POC and SOC concentrations were estimated by the tracer-based method, and other OC (OOC) was obtained by subtracting estimated OC from measured OC.

https://doi.org/10.5194/egusphere-2024-3793
Preprint. Discussion started: 6 January 2025

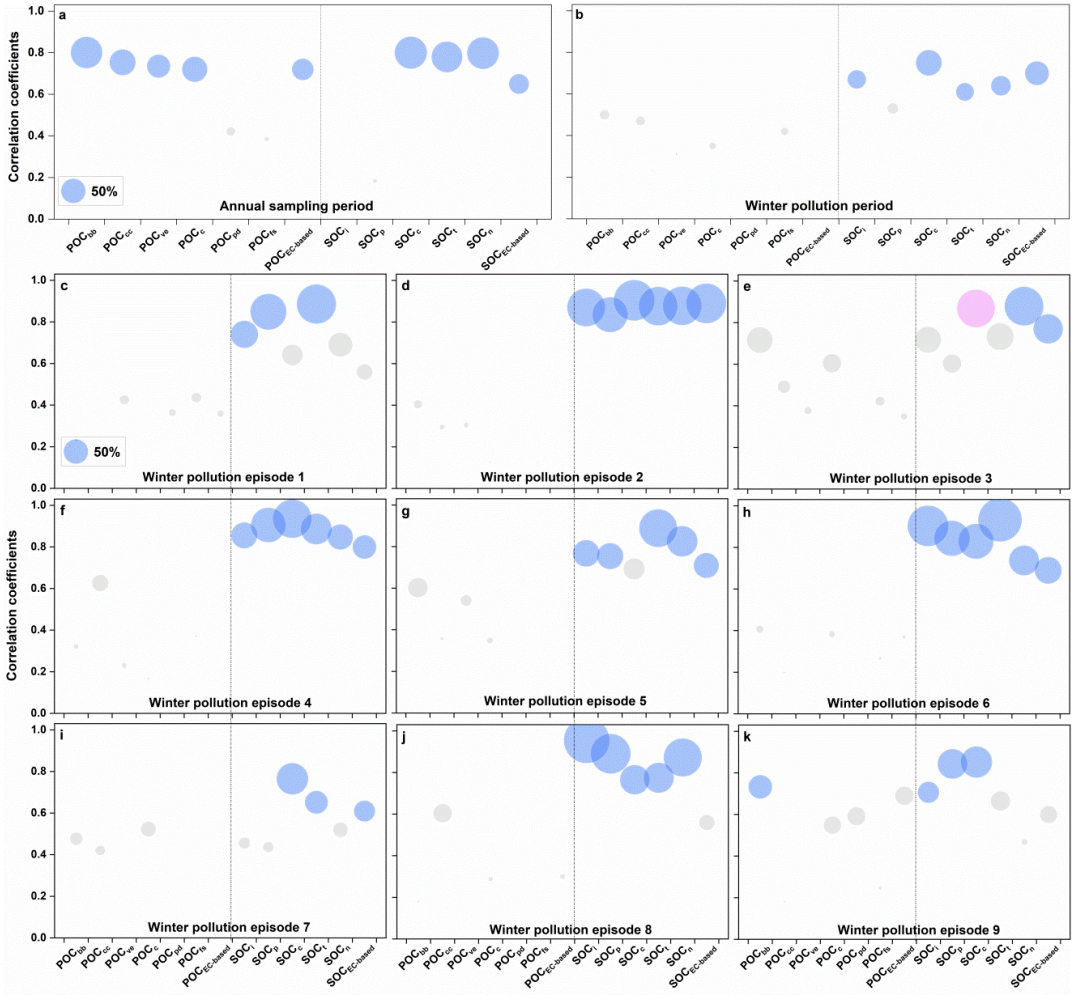

Figure 9. Pearson correlation between POC, SOC, and the measured OC during the annual sampling period and winter pollution episodes. Circle size represents the contribution (%) of POC and SOC to the variation in measured OC, as determined by redundancy analysis. Magenta circles represent P-values from correlation and redundancy analyses that are less than 0.05, while gray circles indicate P-values greater than 0.05. Definitions: POC_{bb} (biomass burning), POC_{cc} (coal combustion), POC_{ve} (vehicle exhaust), POC_{c} (cooking), POC_{pd} (plant debris), POC_{fs} (fungal spores), and $POC_{EC\text{-}based}$ (based on EC method). SOC_{i}, SOC_{p}, SOC_{c}, SOC_{t}, SOC_{n}, and $SOC_{EC\text{-}based}$ refer to SOC from isoprene, α/β-pinene, β-caryophyllene, toluene, naphthalene, and EC-based methods, respectively.

https://doi.org/10.5194/egusphere-2024-3793
Preprint. Discussion started: 6 January 2025

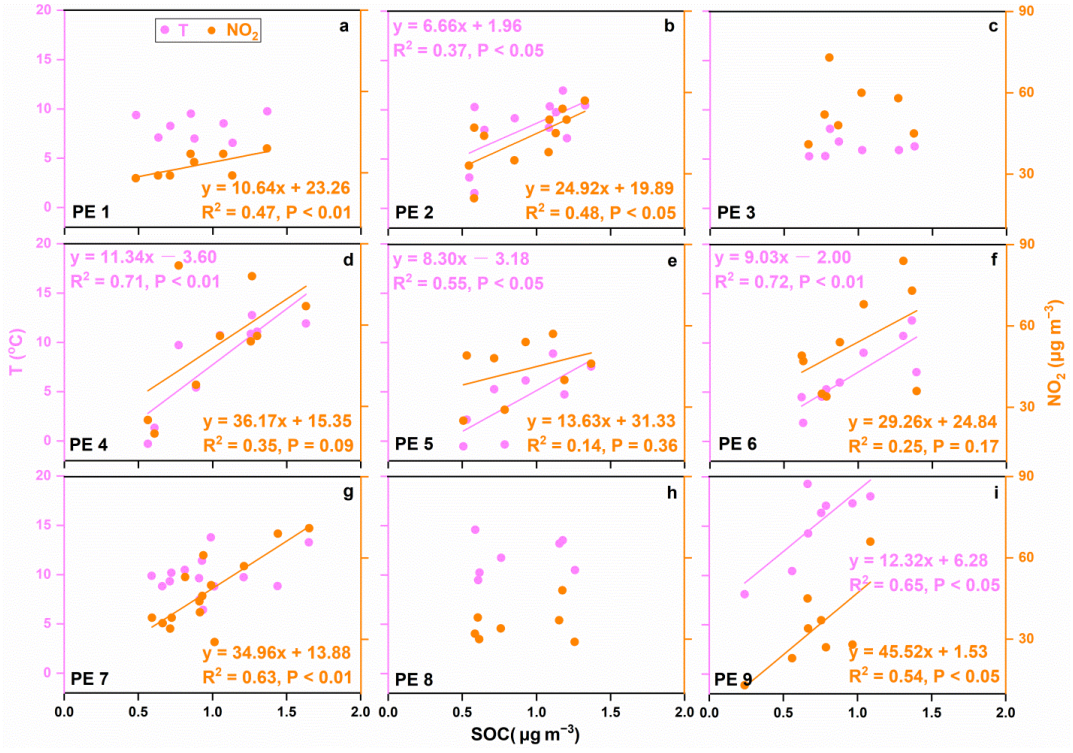

Figure 10. Linear correlation between temperature, NO_2, and SOC during specific winter pollution episode. SOC concentrations were estimated by the tracer-based method.